

TAM  
C6  
CER62-60

~~SECRET~~

COPY 2

██████████  
██████████

EVALUATION OF  
DOMINANT VARIABLES IN DESIGN OF  
EVAPORATOR BODIES

ENGINEERING RESEARCH  
SEP 19 73  
FOOTHILLS READING ROOM

by

L. V. Baldwin  
and  
S. S. Karaki

Prepared for

Stearns-Roger Manufacturing Company  
Denver, Colorado

Colorado State University Research Foundation  
Civil Engineering Section  
Fort Collins, Colorado

October 1962

CER62LVB-SSK60

EVALUATION OF  
DOMINANT VARIABLES IN DESIGN OF  
EVAPORATOR BODIES

by

L. V. Baldwin  
and  
S. S. Karaki

Prepared for

Stearns-Roger Manufacturing Company

Denver, Colorado

Colorado State University Research Foundation  
Civil Engineering Section  
Fort Collins, Colorado

October 1962

CER62LVB-SSK60



U18401 0593877

## SUMMARY

This report presents detailed analyses of the dominate variables affecting vapor release dynamics within an externally heated process evaporator. The rate of bubble growth in a superheated liquid is calculated from a simplified heat transfer theory which is in good agreement with experimental data. This analysis is extended to include the overall energy balance on the process; that is, the final bubble size is approached asymptotically as the slurry feed temperature cools to its saturation value. The rate of escape of these growing bubbles is estimated for the no swirl case by an approximate drag analysis. The net result of these formation and escape dynamics calculations is that approximately 1 second is required for the evaporation to occur in Effect No. 4 with no swirl. This time constant is shown to be very sensitive to the inlet superheat. For example, a drop of  $0.8^{\circ}\text{F}$  in the inlet temperature will not only lower the equilibrium vapor release in direct proportion (i.e. net production drops  $\frac{2.2}{3.0}$  times), but it may take 100 times as long to attain equilibrium in the vessel. Therefore, it seems highly unlikely that evaporator design experience for process equipment with  $10^{\circ}\text{F}$  plus operation is anything but misleading.

The flow field in a turbulent vortex is presented in considerable detail. As a first approximation, the swirling flow has no effect on the fluid residence time at the surface. Thus vortex motion probably neither hinders nor causes "short circuiting" according to the present calculations. However, it must be emphasized that the real outlet or drain geometry was, of necessity, replaced by an idealized, axisymmetric bottom drain in this theoretical treatment. Secondly for a full tangential feed, the slurry surface at the outer wall may be 10 feet higher than at the core of the drain area. The free surface shape is a very sensitive indicator of the turbulence in the flow as well as the swirling velocities.

Finally, a model study is strongly recommended. The first phase of this experimental work would lead to an inlet manifold design which allows for maximum surface-flow residence time. It would also seek to achieve a stable water level thus minimizing wave disturbances which lead to wall crusting. The second phase would test the modeling of evaporation using the analyses for bubble formation and escape presented herein. This series of experiments would be conducted at various superheat inlet temperatures with the actual slurry to be used in the plant equipment. These tests would determine the dominating factor in the evaporation dynamics (be it bubble growth or escape rate), and allow for the reliable extension to plant operating conditions. It is imperative that vapor bubbles be studied in a superheated slurry; air bubbles do not grow at the rate of vapor bubbles (e.g., fig. 2) and entrained air does not have the added mass drag of growing vapor bubbles (see eq. 58a).

## CONTENTS

|   | <u>Page</u> |
|---|-------------|
| SUMMARY . . . . .   | i           |
| CONTENTS . . . . .  | iii         |
| FIGURES . . . . .   | iv          |
| NOMENCLATURE . . . . .  | v           |
| I. INTRODUCTION . . . . .   | 1           |
| 1. Scope of the Study . . . . .   | 1           |
| 2. Description of Evaporator . . . . .                                    | 1           |
| II. QUALITATIVE DISCUSSION OF THE GENERAL PROBLEM. . . . .                | 2           |
| 1. Rotating Flow - Turbulent Field . . . . .                              | 2           |
| 2. Level Slurry Surface - Turbulent Field. . . . .                        | 3           |
| III. THERMAL TRANSPORT RATE AND ENERGY BALANCE. . . . .                   | 4           |
| 1. Required Operating Conditions . . . . .                                | 4           |
| 2. Overall Energy Balance. . . . .  | 4           |
| 3. Surface Evaporation Without Bubble Formation. . . . .                  | 6           |
| 4. Rate of Bubble Growth in a Superheated Liquid . . . . .                | 7           |
| (a) Theory for infinite liquid case . . . . .                             | 7           |
| (b) Experimental data for infinite fluid case . . . . .                   | 10          |
| (c) Theory for finite liquid case . . . . .                               | 11          |
| IV. FLUID VELOCITY FIELD IN A TURBULENT VORTEX . . . . .                  | 13          |
| 1. Simplifying Assumptions . . . . .                                      | 14          |
| 2. Ideal Fluid Case. . . . .  | 15          |
| 3. Laminar Vortex Case . . . . .  | 16          |
| 4. Turbulence Vortex Case. . . . .  | 18          |
| 5. Summary Plots . . . . .  | 19          |
| 6. Scaling the Turbulent Eddy Viscosity (Evaluation of $Re_o$ ) . . . . . | 20          |
| 7. Extension of Vortex Analysis to Cone Geometry . . . . .                | 22          |
| V. BUBBLE ESCAPE RATE . . . . .   | 24          |

CONTENTS

|   | <u>Page</u> |
|---|-------------|
| VI. CONCLUSIONS OF PRECEDING ANALYSIS . . . . . | 27          |
| VII. PROPOSAL FOR MODEL STUDY . . . . .         | 28          |
| 1. Objective of the Model Study . . . . .       | 29          |
| 2. Proposed Method of Study . . . . .           | 30          |
| 3. Time Estimates . . . . .                     | 32          |
| 4. Cost Estimates . . . . .                     | 34          |
| 5. General Comment on Proposal . . . . .        | 35          |
| VIII. ACKNOWLEDGEMENTS . . . . .                | 36          |
| Reference List . . . . .                        | 37          |

## FIGURES

### Figure

|          |  |
|----------|--|
| Sketch A | Elevation View of Cylindrical Evaporator   |
| 1        | Calculated Bubble Radius vs. Time Curves at the Indicated Superheat Temperatures in Water at 1 Atmospheric (Ref. No. 3)  |
| 2        | Experimental Vapor Bubble Growth Rate in 103.1°C Superheated Water at 1 Atmospheric (Ref. No. 3)                         |
| 3a       | Experimental Vapor Bubble Growth Rate (Ref. No. 5)   |
| 3b       | Experimental Data for Bubble Growth in Superheated Water at 1 Atmospheric Ambient Pressure (Ref. No. 4 P. Dergarabedian) |
| 4        | Bubble Growth in Effect No. 4 at Design Superheat ( $\Delta T_{in} = 3.0^{\circ}\text{F}$ )                              |
| 5        | Bubble Growth in Effect No. 4 at 0.73 Times Design Superheat ( $\Delta T_{in} = 2.2^{\circ}\text{F}$ )                   |
| 6        | Sketch for Vortex Flow Analysis  |
| 7        | Tangential Velocity Field in Real Vortex Flow  |
| 8        | Radial Velocity Field in a Vortex Flow   |
| 9        | Eulerian Residence Time in a Vortex Flow   |
| 10       | Shape of Water Surface   |
| 11       | Experimental Tank for the Generation Vortices in a Real Fluid (Ref. No. 8)   |
| 12       | Summary of Evaporation Dynamics Without Swirl  |

NOMENCLATURE

| <u>Symbol</u> | <u>Definition</u>   |
|---------------|---|
| $A_s$ ,       | surface area of liquid interface, $ft^2$ ;                      |
| $B$ ,         | slope of evaporator body, none                                  |
| $C$           | Cavitation Number, none;  |
| $C_{P_L}$ ,   | specific heat of liquid, $\frac{BTU}{lb_m \text{ } ^\circ F}$ ; |
| $f$ ,         | fudge factor, equation 23, none;                                |
| $F$ ,         | Froude Number, none;  |
| $h$ ,         | enthalpy $\frac{BTU}{lb_m}$ ;                                   |
| $h_{fg}$ ,    | latent enthalpy for vaporization, $\frac{BTU}{lb_m}$ ;          |
| $k_L$ ,       | thermal conductivity of liquid, $\frac{BTU}{sec-ft-^\circ F}$ ; |
| $l$ ,         | height of liquid in evaporator, ft;                             |
| $m$ ,         | isolated mass of inlet liquid feed, $lb_m$ ;                    |
| $m_v$ ,       | vapor mass, $lb_m$ ;  |
| $P_o$ ,       | liquid pressure at bubble interface, $\frac{lb_F}{ft^2}$ ;      |
| $P_v$ ,       | vapor pressure inside bubble, $\frac{lb_F}{ft^2}$ ;             |
| $q$ ,         | rate of heat transfer, $\frac{BTU}{sec-ft^2}$ ;                 |
| $Q_{vap}$ ,   | enthalpy of vapor formed after $t$ seconds, BTU;                |
| $R$ ,         | bubble radius, ft (unless otherwise specified);                 |
| $R_o$ ,       | nucleation bubble radius, ft;                                   |
| $R_{max}$ ,   | bubble radius as $t \longrightarrow \infty$ , ft;               |
| $Re$ ,        | Reynolds number, none;  |
| $r$ ,         | radius coordinate in vortex analysis, ft;                       |
| $r_o$ ,       | drain radius of evaporator, ft;                                 |
| $r_w$ ,       | outer wall radius of evaporator, ft;                            |
| $t$ ,         | time, sec;  |
| $T$ ,         | temperature, $^\circ F$ ;                                       |
| $T_L$ ,       | liquid temperature, $^\circ F$ ;                                |
| $T_{in}$ ,    | inlet liquid temperature, $^\circ F$ ;                          |

NOMENCLATURE (cont'd.)

|                   |  |
|-------------------|--|
| $T_o$             | , saturation temperature of liquid, $^{\circ}\text{F}$ ;                   |
| $T_{\infty}$      | , liquid temperature far from bubble, $^{\circ}\text{F}$ ;                 |
| $u$               | , radial liquid velocity, ft/sec;  |
| $u_o$             | , radial liquid velocity at drain, ft/sec;                                 |
| $u_w$             | , radial liquid velocity at well, ft/sec;                                  |
| $v$               | , tangential liquid velocity, ft/sec;                                      |
| $v_o$             | , tangential liquid velocity at drain, ft/sec;                             |
| $v_w$             | , tangential liquid velocity at wall, ft/sec;                              |
| $w$               | , vertical liquid velocity, ft/sec;  |
| $w_B$             | , vertical bubble rise velocity, ft/sec;                                   |
| $\overline{u'v'}$ | , tangential turbulent shear stress velocity, $\text{ft}^2/\text{sec}^2$ ; |
| $v'$              | , ratio of $v/v_w$ , none;   |
| $v'_o$            | , ratio of $v_o/v_w$ , none;   |
| $z$               | , vertical coordinate in vortex analysis, ft;                              |
| $\alpha$          | , weight fraction liquid, none;  |
| $\gamma$          | , specific density of liquid, $\frac{\text{lb}_F}{\text{ft}^3}$ ;          |
| $\Delta$          | , difference, none;  |
| $\epsilon$        | , eddy viscosity, $\frac{\text{lb}_F\text{-sec}}{\text{ft}^2}$ ;           |
| $\theta$          | , tangential coordinate in vortex analysis, radians;                       |
| $K$               | , Karman's constant, 0.3, none;  |
| $\mu$             | , liquid viscosity, $\frac{\text{lb}_F\text{-sec}}{\text{ft}^2}$           |
| $\nu$             | , kinematic liquid viscosity, $\frac{\mu}{\rho}$ , ft/sec <sup>2</sup> ;   |
| $\pi$             | , 3.1416 --  |
| $\rho_L$          | , density of liquid, $\frac{\text{lb}_m}{\text{ft}^3}$ ;                   |
| $\rho_v$          | , vapor density, $\frac{\text{lb}_m}{\text{ft}^3}$ ;                       |
| $\sigma$          | , surface tension constant, $\frac{\text{lb}_F}{\text{ft}}$ ;              |
| $\tau$            | , time constant, sec;  |
| $\tau_F$          | , fluid residence time constant, sec;                                      |
| $\tau_H$          | , bubble formation time constant, sec;                                     |
| $\tau_E$          | , bubble escape time constant, sec;  |

EVALUATION OF  
DOMINANT VARIABLES IN DESIGN OF  
EVAPORATOR BODIES

by

L. V. Baldwin and S. S. Karaki

I. INTRODUCTION

1. Scope of the Study

Evaporation as used in this report, refers to removal of vapor from a superheated liquor solution. Hence, the term evaporator signifies equipment which concentrates liquor solutions. This report is confined to study of a forced-circulation, external heat evaporator. The purpose of the study is to determine the dominant variables to be considered in design of the evaporator body.

2. Description of Evaporator

A schematic diagram of a typical evaporator is shown in sketch A. The brine enters the evaporator near the bottom of the body or vessel. A pump, with the inlet connected near the bottom of the body forces the brine through a steam heat exchanger and the superheated liquid is discharged into the evaporator body. The liquid level in the body is normally above the pump outlet pipe so that the hydrostatic head and pressure in the discharge line tends to suppress boiling in the heat exchanger. Most of the boiling takes place by flashing near the liquor surface in the evaporator body after release from the discharge line.

The rate of forced circulation is large and concentration of the solution is effected by many passes through the heat exchanger. The high rate of circulation has advantages in that:

- (a) High velocity promotes higher rates of heat transfer per unit area of the heat exchanger.
- (b) Wall temperatures are lower, thus causing less decomposition of heat sensitive materials.

- (c) A greater number of effects can be used which amounts to savings on steam.

The evaporator operates under partial vacuum and the concentrated liquor is drawn off a short distance below the vapor liquid interface in the evaporator. The liquor in the evaporator is actually a slurry as crystals are formed in the liquor. Vapor is drawn off at the top of the body.

## II. QUALITATIVE DISCUSSION OF THE GENERAL PROBLEM

A simple mathematical model which adequately describes the dynamic behavior of single or multiple effect evaporators is not feasible.

The total problem involves thermodynamic and hydrodynamic effects in a turbulent, three-dimensional, multiple-phase flow field. The problem is better analyzed theoretically by consideration of separate parts with somewhat simplifying assumptions which do not void the analyses. Such analyses are indicated in the succeeding section.

Since removal of vapor from the superheated brine solution is the principle problem, consideration must be given to the environment which permits maximum vapor release. Other factors involved in the total process which are also affected by environment in the evaporator body are:

- (a) Short circuiting, that is, recirculation of the superheated brine without opportunity for boiling (or flashing).
- (b) Entrainment of liquid and solids in the vapor removed.
- (c) Crystal growth.
- (d) Homogeneous mixing of the slurry.
- (e) Crusting.

### 1. Rotating Flow - Turbulent Field

In a turbulent rotating flow field within the evaporator body, problems arise which while perhaps not directly affecting evaporation, influence some of the other factors itemized above. The tangential entry of the brine into the evaporator body from the discharge line of the pump gives rise to flow rotation, surface waves and splashing in the evaporator pan. This in turn creates deposits of salt along the evaporator wall in a zone above the slurry surface. The rapidity and extent of this wall

crusting depends upon the surface smoothness of the wall, amount of splashing to which the wall area is subjected and entrainment of liquids and solids in the vapor flow upward through the pan. Crusting is the primary operating nuisance since in most instances it requires temporary plant shutdown for removal of the crust in order to avoid damage to the pan. Dynamic unbalanced forces within the evaporator caused by surges and waves can create a problem for structural stability although generally this is of small consequence. The mechanics of vapor formation and release from superheated liquor is discussed in part III of this report. Simplified analyses of vortex motion and effect of cone angle is also discussed in part IV.

## 2. Level Slurry Surface - Turbulent Field

If the slurry surface within the evaporator pan could be maintained relatively level and further if the superheated brine could be introduced into the pan in a thin layer near the vapor slurry interface, evaporation in the pan could be increased. Simultaneously with achieving greater vapor release, waves and splashing would be reduced, entrainment in vapor carry-over also reduced, and a favorable environment could be established for crystal growth and settlement. One way to develop this environment would be to discharge the flow from the recirculating pumps into the pan through a manifold system at low velocities radially from the circumference. Because the vapor bubble must rise through some finite layer of slurry before being released in the vapor space above, the size of the body, in cross-sectional area must be large enough to maintain small downward flow velocity thus permitting the bubbles to rise.

Vapor release from the inlet liquor might also be accomplished if flashing from the superheated liquor could take place in the vapor space of the evaporator pan. This might be accomplished with proper flow entry distribution around its periphery above the slurry-vapor interface, so that there will be minimum splashing and spray carry-over in the vapor outflow. The physical constituents of such a system would have to be determined from model studies and auxiliary equipment such as showers to remove salt deposit would probably be required.

### III. THERMAL TRANSPORT RATE AND ENERGY BALANCE

#### 1. Required Operating Conditions:

The minimum vapor release rate necessary to meet design requirements is calculated in this section and interpreted in terms of bubble size.

- (a) Feed rate is approximately 330,000 gal/min of 15% slurry with superheat\*

$$\frac{3.3 \times 10^5 \text{ gal}}{1 \text{ min}} \times \frac{60 \text{ min}}{1 \text{ hr}} \times \frac{0.134 \text{ ft}^3}{1 \text{ gal}} \times \frac{1.15 (62.4) \text{ lb}_m}{1 \text{ ft}^3} \times \frac{1 \text{ ton}}{2 \times 10^3 \text{ lb}_m} = 95,200 \frac{\text{tons}}{\text{hr}} \quad (1)$$

- (b) Vapor release rate at design value is 179.9 tons/hr

$$(c) P \equiv \frac{\text{Vapor Rate}}{\text{Feed Rate}} = \frac{179.9}{95,200} = 1.89 \times 10^{-3} \frac{\text{lb}_m \text{ vapor}}{\text{lb}_m \text{ feed}} \quad (2)$$

- (d) The corresponding bubble radius  $R$  required to meet design conditions for a single bubble formed in  $m \text{ lb}_m$  of feed is

$$m_v = \frac{4\pi\rho_v}{3} (R^3 - R_o^3) \text{ lb}_m \text{ of vapor}$$

$$P = \frac{m_v}{m} = \frac{4\pi\rho_v}{3} \frac{R^3 - R_o^3}{m} \geq 1.89 \times 10^{-3}$$

so

$$R_{\text{design}} \geq \left[ \frac{3}{4\pi\rho_v} Pm + R_o^3 \right]^{1/3} \geq \left[ \frac{3m}{4\pi\rho_v} (1.89 \times 10^{-3}) + R_o^3 \right]^{1/3} \quad (3)$$

#### 2. Overall energy balance on system of $m \text{ lb}_m$ of isolated, slurry feed with superheat

- (a) The evaporation is a constant enthalpy process

$$h_{\text{total}} = \text{constant} = m C_{pL} (T_{\text{in}} - T_o) \quad (4)$$

where  $m$  = weight of inlet feed used as a basis of calculation

$T_{\text{in}}$  = inlet liquid feed temperature

\*Superheat is defined as a condition of a liquid which is warmer than  $T_o$  with a surface or ambient pressure  $P_o$ ;  $P_o$  is the vapor pressure at  $T_o$ .

$T_o$  = saturation temperature of liquid at the surface pressure.

At any instant after the feed enters, this energy balance is

$$h_{total} = m \alpha C_{P_L} (T_L - T_o) + m(1-\alpha)h_{fg} \quad (5)$$

where  $\alpha$  = weight fraction liquid  
 $1-\alpha$  = weight fraction vapor  
 $h_{fg}$  = latent heat of vaporation at  $T_o$

this may be written as,

$$T_L = \frac{\frac{h_{tot}}{m} - (1-\alpha) h_{fg}}{\alpha C_{P_L}} + T_o \quad (6)$$

now let us relate the fraction of vapor formed to the single bubble radius

$$Q_{vap} = \int_0^t q \, dt = h_{fg} \frac{4\pi\rho_v}{3} (R^3 - R_o^3) = m(1-\alpha) h_{fg}$$

$$\text{or } m(1-\alpha) = \frac{4\pi\rho_v}{3} (R^3 - R_o^3) \quad (7)$$

The overall energy balances written in this section implicitly assumes that all of the heat of vaporization enters as superheated slurry from the heat exchangers. In fact, a more careful analysis shows that approximately 10% of this energy enters as a hot brine feed line (No. 152) and another 4% in the same inlet (No. 3). However, we can as an approximation assume that these heat sources act as a preheater for the circulating slurry. This simplified approach was used herein.

(b) Clearly the evaporation is completed, and the bubble radius therefore a maximum, where all of the inlet superheat has gone to form vapor. That is,  $R_{max}$  occurs when

$$h_{total} = m(1-\alpha)_{max} h_{fg}$$

so 
$$h_{total} = \left(\frac{4\pi\rho_v}{3}\right) (R_m^3 - R_o^3) h_{fg}$$

and

$$R_{\max} = \left[ \left( \frac{3}{4\pi\rho_v} \right) \frac{h_{\text{tot}}}{h_{fg}} + R_o^3 \right]^{1/3} \quad (8)$$

This is an important result. We expect that any rate of heat transfer solution which we formulate for the bubble growth will have  $R_{\max}$  as a  $t \longrightarrow \infty$  asymptote. Secondly, recalling the vapor release requirements for design conditions, we can write

$$R_{\max} \geq R_{\text{design}}$$

assuming the design is for equilibrium vapor release,

$$R_{\max} \simeq R_{\text{design}} \quad (9)$$

so

$$\frac{3}{4\pi\rho_v} \frac{h_{\text{tot}}}{h_{fg}} + R_o^3 \simeq \frac{3}{4\pi\rho_v} P_m + R_o^3$$

$$\frac{h_{\text{total}}}{h_{fg}} \simeq P_m \quad (10)$$

or

$$\frac{h_{\text{total}}}{m} \simeq P h_{fg} \quad (11)$$

which checks; all inlet superheat must go out as overhead vapor.

### 3. Surface Evaporation Without Bubble Formation

The vaporation from a liquid surface has never been treated under reduced pressure or vacuum flows satisfactorily. However, there is no doubt that at least a fraction of the vapor outflow comes from surface evaporation without boiling. A comprehensive and critical survey of "evaporation coefficients" is available in reference 1. We can make a very rough estimate as follows:

$$\frac{m_v}{A_s} = \alpha_E \frac{P_v}{\sqrt{2 \pi R_G T}} \quad (12)$$

Unfortunately although we can use the "accepted" value of  $\alpha_E = 0.04$ , we must expect  $\alpha_E$  to be a function of the apparatus design rather than

a true physical constant. Using the equilibrium vapor pressure of 1.2 psi,

$$m_v = \frac{\alpha_{E_v} p A_s}{\sqrt{\frac{2 \pi R_G T_L}{M}}}$$

or numerically for Effect No. 4,

$$m_v = \frac{0.04 (1.2 \times 144) \left( \frac{\pi}{4} \times 33.5^2 \right)}{\sqrt{\frac{2 \times 3.14 \times 1546 \times 585}{18 \times 32.2}}}$$

that is,  $m_v = 59.5 \text{ lb}_m/\text{sec} = 107.2 \frac{\text{tons}}{\text{hr}}$  (per effect) (13)

This rough estimate shows that we might expect up to the total design evaporation rate to take place at the surface without boiling. However, since the "constant"  $\alpha_E$  is actually dependent on the absolute pressure level, the overhead geometry, and the thermal conditions just below the slurry surface, it would be unwise to rely on this estimate. This surface evaporation rate might best be considered a "safety factor" in a design which is based on bubble growth and escape dynamics, because it is the absolute upper limit attainable by this mode.

#### 4. Rate of Bubble Growth in a Superheated Liquid

##### (a) Theory for infinite liquid case:

Fortunately considerable theoretical work has been published on the dynamics of bubble growth in pure superheated liquids. A recent series of experiments has considerably clarified the physics; we now can choose a suitably simplified model, calculate bubble growth rate almost quantitatively, and be reasonably certain of our results.

This section will outline the theory, cite the experimental evidence, then extend the analysis by some original work to thermal conditions which might be encountered in evaporator design.

When the vapor pressure in a liquid exceeds the ambient pressure, it is possible for a vapor bubble to grow. This initial formation is called nucleation; this portion of the physics is subject to much speculation but

no experimental observations. However, it is generally believed that this nucleus is a region of non-liquid phase such as a dissolved gas or a solid particle. Since we are dealing with a slurry, nucleation is of no practical concern. However, to avoid possible confusion, the equations commonly used for the nucleation phase of bubble growth are outlined herein. It turns out that virtually every research paper on bubble growth rehashes this theory (due to Lord Rayleigh) and by briefly reviewing it, we hope to put it in proper perspective. According to Rayleigh's theory, the growth of a vapor bubble is controlled by the three factors: inertia of the bubble, the surface tension, and the vapor pressure. As the bubble grows, evaporation takes place at the bubble boundary; the heat necessary for this evaporation comes from the liquid at the bubble wall, and to a lesser extent the bubble vapor. So as the growth cools the liquid interface, the vapor pressure in the bubble decreases correspondingly. The heat inflow requirement for evaporation is dependent on bubble growth rate, so this problem is complex and requires the simultaneous solution of fluid dynamical and heat transfer differential equations. The relative velocity of the bubble to the surrounding fluid is initially small; therefore, the heat flow problem is formulated as a molecular diffusion of heat to a growing, isothermal sphere. A quantitative formulation of the dynamic problem can be found in references 2, 3, 4 and 5. The net result is that growth of vapor bubbles in superheated liquids is found to be controlled by this thermal transport of heat from the distant fluid to the bubble wall. All observations on real vapor bubbles are in good agreement with the bubble radius-time behavior predicted by a greatly simplified heat transport theory. These experiments in water show no explicit dependence of bubble growth on hydrostatic head or depth of liquid level. This point will be further discussed after the theoretical review.

The physical model assumes a spherical vapor bubble at uniform temperature and pressure. The temperature of the vapor is that of the liquid at the bubble wall, and the pressure is the equilibrium vapor pressure for that temperature. In addition, the effects of viscosity and compressibility are neglected both in the vapor and in the liquid. Reference 3 gives a detailed apologetics of these simplifications; most convincing arguments are the data summarized later.

Lamb (ref. 6) gives the equation of motion of a bubble of radius  $R$  in a non-viscous, incompressible (i.e., ideal) liquid as a function of time:

$$R \frac{d^2R}{dt^2} + \frac{3}{2} \left( \frac{dR}{dt} \right)^2 = \frac{[p(R) - P_0]}{\rho_L} \quad (14)$$

where  $P_0$  is the "external pressure" (actually for the ideal fluid it is the pressure at infinity), and  $p(R)$  is the pressure in the liquid at the bubble boundary. The pressure  $p(R)$  is rewritten in terms of the vapor pressure and surface tension  $\sigma$  as follows:

$$p(R) = p_v(T) - \frac{2\sigma}{R} \quad (15)$$

Taking  $\sigma$  and  $\rho_L$  as constants, we can introduce a radius  $R_0$  which is the effective initial radius of the nucleus:

$$\frac{2\sigma}{R_0} = p_v(T_0) - P_0 \quad (16)$$

The Rayleigh solution is the long time asymptotic solution of equation 14 where it is assumed that the cooling effect of evaporation can be neglected. That is,  $p_v(T) = p_v(T_0) = \text{constant}$ . For  $R \gg R_0$ , the solution is (ref. 3):

$$\frac{dR}{dt} \simeq \sqrt{\frac{4\sigma}{3\rho_L R_0}} = \sqrt{\frac{2}{3\rho_L} [p_v(T_0) - P_0]} \quad (17)$$

The bubble growth is unlimited;  $R$  increases linearly with time  $t$  proportional to a physical constant group. The actual bubble growth rate deviates markedly from the Rayleigh solution because of the cooling effect. (This equation may apply to permanent gas bubbles like air in water where  $p_v(T) = p_{\text{air}}$ , and it may also apply to the initial nucleation of a vapor bubble.)

At this point of the analysis, Plesset and Zwick (ref. 3) set up the heat transfer rate equation to a growing sphere in a stagnant liquid. They use the complicated solution for liquid interface temperature obtained in reference 2 in the form of liquid wall temperature as a function of  $R$  and  $\frac{dR}{dt}$ . They solve equation 14 simultaneously with this heat transfer equation;

that is, they use  $p_v(T)$  matched correctly to  $T$  for the instantaneous bubble size and growth rate. Their final solution for radius  $R$  versus time  $t$  is obtained with considerable effort, but for  $R \gg R_0$  (which is the case of interest if one is interested in evaporation), the equation is:

$$\frac{dR}{dt} \approx \left(\frac{3}{\pi}\right)^{1/2} \frac{k_L (T_\infty - T_0)}{\rho_L h_{fg} \sqrt{\left(\frac{k}{\rho C_P}\right)_L}} \frac{1}{\sqrt{t}} \quad (18)$$

That is, the rate of bubble growth depends on some thermal transport properties of the liquid, the liquid superheat and the rate diminishes with increasing time. Figure 1 shows typical calculated bubble histories.

(b) Experimental data for infinite fluid case:

Experimental evidence in the form of high speed photographs of bubbles growing in water (and other liquids) was published by Dergarabedian (ref. 4 and 5). He superheated pure liquids using sun lamps to carefully define a uniform temperature region in a tube of liquid. Figure 2 compares his results with both the Rayleigh solution (eq. 17) and the complete heat transfer result of Plesset and Zwick (eq. 18). The agreement is remarkable. In fact, the only data "adjustment" was a slight (+ 0.002 sec.) shift of the time scale to allow for the fact that bubbles smaller than  $10^{-2}$  cm are not visible and hence  $t = 0$  is somewhat uncertain. To check the generality of predictions concerning physical constants, the results of figure 3 are included.

The only allowance for pressure variation on bubble growth is the dependence of  $T_0$ , the saturation temperature of the liquid at the bubble interface, on the ambient or liquid free-surface external pressure. Since we are considering the formation and release due to buoyant forces of a bubble within a relatively short time, and since the referenced experiments were actually performed under 1/2 foot heads, the growth equation probably is reliable. It simply can not be applied directly to fluid under large hydrostatic head.

(c) Theory for finite liquid case:

The result for bubble growth (eq. 18) however as it stands represents an unattainable maximum for process evaporation design. Equation 18 assumes that  $(T_\infty - T_0)$  is constant; it applies to a single bubble formed at that superheat in an infinite volume of liquid. As a first step in the adaptation of this thermal transport limitation on bubble growth, we will give an extremely simple formulation of the Plesset-Zwick result.

$$\left\{ \begin{array}{l} \text{Rate of Heat Conduction} \\ \text{of Liquid, } q_c \end{array} \right\} = \left\{ \begin{array}{l} \text{Rate of Accumulation of} \\ \text{Latent Heat in Bubble,} \\ q_E \end{array} \right\} \quad (19)$$

The heat conduction is easy to formulate rigorously but difficult to solve except by numerical or machine computation due to the time varying bubble interface (ref. 2). As an approximation, assume that all of the temperature drop causing conduction occurs in a growing "thin thermal boundary" of thickness  $f \sqrt{\left(\frac{k}{\rho C_P}\right)_L t}$ . So,

$$q_c = k_L \frac{(T_\infty - T_0)}{f \sqrt{\left(\frac{k}{\rho C_P}\right)_L t}} 4\pi R^2 \quad (20)$$

That is, the rate of heat conduction through the liquid is proportional to the product of liquid thermal conductivity and bubble surface area; the superheat "driving force" acts across a thermal resistance length. Note that  $f$  stands for "fudge factor" to be determined soon.

By contrast, the latent enthalpy of the bubble is obtained more directly:

$$q_E = h_{fg} \frac{d}{dt} \left( \frac{4\pi R^3 \rho_v}{3} \right) \quad (21)$$

Reference 3 shows that  $\frac{d\rho_v}{dt} \approx$  zero. So combining equations 19 and 20 with 21 yields:

$$\frac{dR}{dt} = \frac{k_L (T_\infty - T_0)}{f \rho_L h_{fg} \sqrt{\frac{k}{\rho C_P}}_L} \frac{1}{\sqrt{t}} \quad (22)$$

Comparing with the "exact" formulation solution of the motion dynamics and heat transfer (eq. 18), we see that the "fudge factor" was hardly necessary.

$$f = \sqrt{\frac{\pi}{3}} \approx 1.02 \quad (23)$$

This re-assuring result is the starting point of extension to finite liquid feed rates.

Physically, we are interested in the formation and growth rate of a single bubble in a finite mass of superheated liquid. Previously in the overall energy balance, we used a basis of  $m \text{ lb}_m$  of feed. Now by assuming that the liquid is well-mixed, we can write the temperature driving force for bubble growth in a finite liquid as follows:

$$T_L - T_O = T_\infty - T_O$$

but from the overall energy balance, equation 6 we have:

$$T_\infty - T_O = \frac{h_{\text{tot}} - (1-\alpha) h_{fg}}{\alpha C_{P_L}} \quad (6)$$

or writing this in terms of bubble radius from equation 7, this driving force is:

$$T_\infty - T_O = \frac{h_{\text{tot}} - \frac{4\pi\rho_v}{3} (R^3 - R_O^3) h_{fg}}{C_{P_L} \left[ m - \frac{4\pi\rho_v}{3} (R^3 - R_O^3) \right]} \quad (24)$$

With this substitution, bubble growth equation for a single bubble in a finite liquid is:

$$\frac{dR}{dt} = \sqrt{\frac{\pi}{3}} \frac{\sqrt{(k \rho C_P)_L}}{\rho_v h_{fg}} \frac{1}{\sqrt{t}} \left\{ \frac{h_{\text{tot}} - \frac{4\pi\rho_v}{3} (R^3 - R_O^3) h_{fg}}{C_{P_L} \left[ m - \frac{4\pi\rho_v}{3} (R^3 - R_O^3) \right]} \right\} \quad (25)$$

This equation can be solved for the bubble radius  $R$  as a function of time  $t$  by separation of variables. The resulting new expression for bubble growth (after considerable re-arranging) is:

$$\sqrt{\frac{\pi}{3}} \frac{\rho_v}{\rho_L} \frac{1}{\sqrt{\left(\frac{k}{\rho C_P}\right)_L}} \left[ R + \frac{1}{3} R_{\max} \left( 1 - \frac{m}{(m_v)_{\max}} - \frac{R_0^3}{R_{\max}^3} \right) \right] \cdot \left\{ \sqrt{3} \arctan \frac{2R+R_{\max}}{-\sqrt{3} R_{\max}} + \ln e \left| \frac{R-R_{\max}}{\sqrt{R_{\max}^2 + R R_{\max} + R^2}} \right| \right\} = 2 \sqrt{t} \quad (26)$$

This expression shows that the growth depends on the ratio of vapor to liquid density, the thermal diffusivity of the liquid and the ratios of initial feed mass to final vapor mass, and initial bubble nuclei radius to final bubble radius. This maximum bubble radius  $R_{\max}$  is approached as  $t \rightarrow \infty$ ;  $R_{\max}$  is given by the overall energy balance, equation 8.

Several plots of this bubble growth equation have been prepared and are included as figures 4 and 5. Now like all rate approaches to an equilibrium condition, these plots show that the maximum vapor release takes an infinitely long time. But for all practical purposes the evaporation is complete when  $R = 0.95 R_{\max}$ . Taking this definition as the required thermal residence time  $\tau_H$  required, we see that for the proposed design conditions of Effect No. 4,  $\tau_H = 300$  to 3 milliseconds depending on the volume of liquid feed from which the vapor is formed.

#### IV. FLUID VELOCITY FIELD IN A TURBULENT VORTEX

This section summarizes what analyses are available for incompressible turbulent vortex flows, applies and extends the theory to the proposed evaporator design geometry, and summarizes the Eulerian flow field in a series of figures. It must be emphasized at the outset however that, although this theoretical treatment has engineering utility, the direct use of this section's results in real evaporator design is unwise without pilot model tests. The reasons for this limitation will be made clear in the subsequent paragraphs.

A good survey of recent work in swirling incompressible flow is available as reference 7. Of the articles discussed, the one which best

fits our needs was published by H. A. Einstein (ref. 8 and 9). The initial part of this section draws heavily on Einstein's work, supplemented by the analysis of Deissler (ref. 10). The extension of this work to the cone-shaped evaporator body is original, as are the Eulerian residence time and fluid field plots.

1. Simplifying Assumptions for Mathematical Formulation of the Problem:

A real turbulent vortex is a very complicated three-dimensional problem. At the outset, we idealize the physics as follows:

(a) Referring to figure 6, the vortex axis is assumed to coincide with the vertical axis of a cylindrical Cartesian coordinate system.

(b) The flow pattern is assumed to be symmetric to the z-axis.

(c) Average velocity components in the z-direction are assumed to be negligible.

(d) The change of water depth at the vortex core is assumed to be small compared to the total water depth; so the radial velocity  $u$  is calculated as though  $h = \text{constant}$ .

At the outset then, we picture a steady vortex in figure 6 which is being fed uniformly at the outer edge with liquid. Furthermore, this outer inlet flow comes in fully tangent at the outer wall over the entire depth.

Secondly, all liquid is withdrawn from an axially placed drain at the same mass rate at which fluid is fed at the outer wall. All flow patterns are the same at any depth by our initial assumptions. Then noting again that all coordinate directions and mean velocity components are defined in figure 6, we can write the Navier-Stokes equations for fluid dynamics as follows:

$$\frac{D'u}{Dt} - \frac{v^2}{r} = -\frac{1}{\rho} \frac{\partial}{\partial r} (p + \gamma h) + \nu (\nabla^2 u - \frac{u}{r^2} - \frac{2}{r^2} \frac{\partial v}{\partial \theta}) \quad (27)$$

$$\frac{D'v}{Dt} + \frac{uv}{r^2} = -\frac{1}{\rho} \frac{1}{r} \frac{\partial}{\partial \theta} (p + \gamma h) + \nu (\nabla^2 v + \frac{2}{r^2} \frac{\partial u}{\partial \theta} - \frac{v}{r^2}) \quad (28)$$

$$\frac{D'w}{Dt} = -\frac{1}{\rho} \frac{\partial}{\partial z} (p + \gamma h) + \nu (\nabla^2 w) \quad (29)$$

the continuity equation completes the set:

$$\frac{1}{r} \frac{\partial}{\partial r} (ru) + \frac{1}{r} \frac{\partial v}{\partial \theta} + \frac{\partial w}{\partial z} = 0 \quad (30)$$

where the operators and new symbols are:

$$\begin{aligned} \frac{D'}{Dt} &= \frac{\partial}{\partial t} + u \frac{\partial}{\partial r} + \frac{v}{r} \frac{\partial}{\partial \theta} + w \frac{\partial}{\partial z} \\ \nabla^2 &= \frac{\partial^2}{\partial r^2} + \frac{1}{r} \frac{\partial}{\partial r} + \frac{1}{r^2} \frac{\partial^2}{\partial \theta^2} + \frac{\partial^2}{\partial z^2} \end{aligned}$$

and  $\nu$  = liquid kinematic viscosity

$\rho$  = liquid density (subscript L omitted in this section only)

$\gamma$  = specific weight of the liquid

$p$  = the liquid pressure.

We will examine the solutions in increasing order of their complexity, then summarize the experimental findings. The last section is devoted to scaling laws of the turbulent eddy viscosity and cone-shaped body designs.

## 2. Ideal Fluid Case

Outside the drain area; i.e.,  $r > r_0$ .

Here we take,  $v = 0$  and  $u \neq f(z) \neq f(\theta)$

$$w = 0 \quad v \neq f(z) \neq f(\theta)$$

Also due to assumptions initially made,  $\frac{\partial}{\partial t} = \frac{\partial}{\partial \theta} = \frac{\partial}{\partial z} = 0$ .

Equations 27, 28, and 30 become:

$$-\frac{\partial}{\partial r} \left( \frac{u^2}{2} \right) + \frac{v^2}{r} = \frac{1}{\rho} \frac{\partial}{\partial r} (p + \gamma h) \quad (27a)$$

$$u \frac{\partial v}{\partial r} + \frac{uv}{r} = 0 \quad (28a)$$

$$\frac{\partial}{\partial r} (ru) = 0 \quad (30a)$$

The first (and the most general) result obtained comes from the reduced continuity equation, (30a).

$$\frac{\partial}{\partial r} (ru) = 0 \quad \text{or} \quad ru = \text{constant}. \quad (31)$$

Thus, the radial discharge outside the drain area is constant;

$$Q_{in} = 2\pi r l u \quad (32)$$

or

$$ru = \frac{Q_{in}}{2\pi l} \quad (33)$$

For this zero viscosity case, equation 28a can be integrated directly.

$$vr = \text{constant} \quad (34)$$

So the inlet moment of momentum,  $v_w r_w$  is conserved in the absence of viscosity.

Inside the drain area; i.e.,  $r < r_0$ .

The tangential velocity solution is unchanged; equation 34 still applies although it gives a physically impossible singularity at the center axis where  $v \rightarrow \infty$  as  $r \rightarrow 0$ .

The radial solution from continuity allows for a uniform outflow (i.e.,  $w = \text{constant}$  within  $r < r_0$ ). So equation 30a becomes,

$$\frac{\partial}{\partial r} (ru) + \frac{Q_0}{2\pi l r_0^2} \quad r = 0 \quad (35)$$

where  $l$  is the length of the chamber at the core. Integrating this expression with the assumed boundary conditions yields,

$$Q_r = Q_0 \frac{r^2}{r_0^2} \quad (36)$$

where  $Q_r = -2\pi l ru = \text{discharge occurring within } r$ . Furthermore, since this result is a result of continuity only, it is generally true for all viscosities.

### 3. Laminar Vortex Case

Inside the drain area; i.e.,  $r < r_0$ . With the previously stated simplifications and continuity results, equation 27 becomes:

$$u \frac{\partial u}{\partial r} - \frac{v^2}{r} = -\frac{1}{\rho} \frac{\partial}{\partial r} (p + \gamma h) + v \frac{\partial}{\partial r} \left( \frac{1}{r} \frac{\partial (ur)}{\partial r} \right) \quad (37)$$

Recalling that for  $r < r_0$ ,

$$u = - \frac{Q_r}{2 \pi r \ell} = - \frac{Q_o r}{2 \pi r_o^2 \ell}$$

then the last term which represents radial shear becomes

$$\frac{1}{r} \frac{\partial(ur)}{\partial r} = \frac{Q_o}{\pi r_o^2 \ell} = \text{constant} \quad (38)$$

So the viscous component equation of radial momentum given above (eq. 37) reduces to the form given for ideal fluids. That is,

$$- \frac{\partial}{\partial r} \left( \frac{u^2}{2} \right) + \frac{v^2}{r} = \frac{1}{\rho} \frac{\partial}{\partial r} (p + \gamma h) \quad (27)$$

Equation 27 is very helpful in enabling us to interpret experiments where the free surface shape of the vortex is observed. This point is clarified later.

The radial velocity equation simplifies to the following:

$$u \frac{\partial v}{\partial r} + \frac{uv}{r} = v \left( \frac{\partial^2 v}{\partial r^2} + \frac{\partial v}{\partial r} - \frac{v}{r^2} \right) \quad (39)$$

This equation can be integrated directly for  $v = f(r)$  since we already have  $u = f'(r)$  from continuity. The integration constants assume that the inlet tangential momentum to this drain core is  $v_o r_o$ ; and at  $r = 0$ , we require that this moment of momentum be zero due to viscosity (thereby avoiding infinite velocities). The final solution may be written as:

$$\frac{v r}{v_o r_o} = \frac{1 - e^{-\frac{Re_o}{2} \left( \frac{r}{r_o} \right)^2}}{1 - e^{-\frac{Re_o}{2}}} \quad (40)$$

The new important parameter in this solution is a radial flow Reynolds Number evaluated at the drain radius section.

$$Re_o \equiv \frac{u_o r_o}{\nu} \quad (41)$$

Again since the vertical static pressure distribution is of no interest for our study, we do not examine the z-component result.

Outside of drain area;  $r > r_o$ .

The solution of the tangential component equation 39 requires modified boundary conditions. These are that the inlet moment of momentum at the other wall radius  $r_w$  will be  $v_w r_w$  and that this solution match equation 40 at  $r = r_o$ . The resulting expressions are:

$$\left. \begin{aligned} r'v' &= \left[ \frac{r'_o v'_o - r'_o^{-(Re_o-2)}}{1 - r'_o^{-(Re_o-2)}} \right] \left( 1 - r'^{-(Re_o-2)} \right) + r'^{-(Re_o-2)} & Re_o \neq 2 \\ r'v' &= 1 + (v'_o r'_o - 1) \frac{\ln_e r'}{\ln_e r'_o} & Re_o = 2 \end{aligned} \right\} \quad (42)$$

All the primes indicate non-dimensional values where the reference radius is  $r_w$  and the reference velocity is  $v_w$ ; as always, the sub zero indicates a value for the drain radius position  $r = r_o$ .

To find the absolute value of  $v_o$  at  $r_o$ , we require that the  $v$  vs  $r$  curve be smooth, so that  $\frac{\partial}{\partial r} \left( \frac{v}{r} \right)$  at  $r = r_o$  is equal from both equations 40 and 42. The final results are:

$$\left. \begin{aligned} v'_o &= \frac{1}{r'_o} \left[ \frac{(Re_o - 2) (1 - e^{-Re_o/2})}{Re_o \left( 1 - e^{-Re_o/2} r'_o^{(Re_o-2)} - 2 (1 - e^{-Re_o/2}) \right)} \right] & Re_o \neq 2 \\ v'_o &= \frac{1}{r'_o} \left[ \frac{1 - e^{-1}}{1 - e^{-1} - 2 e^{-1} \ln_e r'_o} \right] & Re_o = 2 \end{aligned} \right\} \quad (43)$$

Therefore, equations 40 and 42 coupled with equation 43 represent the formal solution of tangential velocity as a function of radius for a single laminar vortex.

#### 4. Turbulent Vortex Case

The algebra necessary to obtain this solution is lengthy but the results may be summarized rather concisely.

The u-component solution versus  $r$  is again equations 31 and 36 for the two regions inside or outside of the drain radius.

By letting

$$v = \underbrace{\bar{v}}_{\substack{\text{steady} \\ \text{value}}} + \underbrace{v'}_{\substack{\text{fluctuating} \\ \text{value}}}; \quad u = \bar{u} + u'; \quad w = \bar{w} + w'$$

Equation 39 becomes

$$\bar{u} \frac{\partial \bar{v}}{\partial r} + \frac{\bar{u} \bar{v}}{r} = \nu \left( \frac{\partial^2 \bar{v}}{\partial r^2} + \frac{1}{r} \frac{\partial \bar{v}}{\partial r} - \frac{\bar{v}}{r^2} \right) - \frac{\partial}{\partial r} (\overline{u'v'}) - 2 \frac{\overline{u'v'}}{r} \quad (44)$$

The solution of this equation is formally impossible due to too many unknowns. But the turbulent momentum transfer terms may be assumed to be described by an "eddy viscosity"  $\epsilon$ . Einstein (ref. 8) shows that by letting:

$$\epsilon r \frac{\partial}{\partial r} \left( \frac{v}{r} \right) = - (\overline{u'v'}) \quad (45)$$

and  $\epsilon = \text{constant}$

then the effect of turbulence is simply to act as a numerically larger viscosity. Therefore, equations 40, 42 and 43 apply if we define the Reynolds number as follows:

$$Re_o = \frac{u_o r_o}{(\epsilon + \nu)} \quad (41a)$$

## 5. Summary Plots

To summarize the simplified vortex flow solutions, figures 7 to 10 were prepared. These curves for  $v$  vs  $r$  show the two limiting cases.  $Re_o = 0$  corresponds to a "solid wheel flow"; eddy viscosity is in the limit of  $\epsilon \longrightarrow \infty$  enough to cause the vortex to behave as a solid body rotation. The  $Re_o = \infty$  curve corresponds to the inviscid vortex flow. Except at the lower  $Re_o$ , the curves tend to approach the inviscid flow line ( $v/v_o = r_o/r$ ) in the wall region, whereas they approach the wheel flow near the center. It seems safe to say in general that the outer region is governed by inertia effects, whereas near the center the viscous effects become more important.

The conclusion for any particular case clearly depends on the exact value of  $Re_0$ . The laminar  $Re_0$  for the proposed design of the evaporator shell is noted on these plots. However, the actual flow will be highly turbulent and to characterize it, we must know the "eddy viscosity"  $\epsilon$ . Before attempting to estimate this flow field "fudge factor" it is important to seek experimental justification for equation 45.

Li (ref. 9) photographed the water surface shape for the apparatus sketched in figure 11. He found that the observed surface was well described by the solution of equation 27 using the  $u$  and  $v$  radial variations, shown in figures 7 and 8 for  $Re_0 \approx 2$  to 5. Since  $\frac{\partial}{\partial r}(p + \gamma h)$  is the slope of the free water surface, equation 27 does describe this surface when  $u$  and  $v$  are known. Li concluded that the assumption of constant eddy viscosity (eq. 45) was adequate for his real water vortex flows. Secondly, he found that the flow was highly turbulent ( $Re_0 < 5$ ). However, it is impossible to "scale" these results to evaporator conditions directly.

#### 6. Scaling the Turbulent Eddy Viscosity (Evaluation of $Re_0$ )

R. G. Deissler is one of the most successful practitioners in the art of mixing-length theory. In reference 10, he attempts to predict the eddy viscosity by using von Karman's similarity hypothesis which has been successful for flows through tubes. He assumes that the turbulence at a point is dependent only on the shearing deformation at the point and in the vicinity at that point. Karman's analysis assumes that:

$$\epsilon = \frac{-K \left( \frac{dv}{dr} - \frac{v}{r} \right)^3}{\left[ \frac{d}{dr} \left( \frac{dv}{dr} - \frac{v}{r} \right) \right]^2} \quad (46)$$

Since we assumed that  $Re_0$  is uniform,  $\epsilon$  is constant throughout the vortex. In pipe flow  $K$  has been found to be approximately 0.3 to 0.4. As a first approximation, the derivatives in equation 46 can be evaluated by assuming that;

$$v = \frac{v_w r}{r}$$

The justification for this is figure 7 which shows that except for the lowest  $Re_o$  values and in the drain core region (which has a small total area)  $v$  is roughly described by the ideal fluid case ( $Re_o = \infty$ ). With this rough approximation, equation 46 becomes

$$\epsilon = \frac{(0.3)^2 v_w r_w}{2} \quad (47)$$

and

$$Re_o = - \frac{2}{(0.3)^2} \frac{u_w}{v_w} \quad (48)$$

Recalling that

$$u_w = \frac{-Q}{2\pi r_w l}$$

and that

$$v_w = \frac{Q}{\pi (r_{inlet})^2 n_{inlet}}$$

we get that for a cylindrical simplified turbulent vortex flow,

$$Re_o \simeq \frac{n_{inlet} (r_{inlet})^2}{0.09 r_w l} \quad (49)$$

This is an important result despite all idealizations made in its development, for it shows that for a typical evaporator design:

$$Re_o = \frac{3 \left(\frac{42}{12}\right)^2}{0.09 (16.8) (20)} \simeq 1.9 \quad (50)$$

independent of mass flow rate! Recalling the flow field figures 7 to 10, this result implies: (1) that the free surface may rise as much as 10 feet at the wall compared with the core surface; (2) that the geometric scaling of the Eulerian flow field should be possible and as a first approximation governed by equation 50; (3) that the free surface observations are very sensitive indicators of swirl and turbulence; (4) that any buoyant body force acting in the radial direction on the vapor bubble will best be approximated by:

$$\text{centrifugal acceleration} = \frac{v^2}{r} \propto \frac{1}{r^3} \quad (r > r_o)$$

but (5) that in the regions of the drain core this radial acceleration

is greatly damped by turbulent and for  $r < r_0$ ,  $\frac{v^2}{r} \propto r$ .

### 7. Extension of Vortex Analysis to Cone Geometry

The previous simplified analysis of a single vortex in a real fluid was largely possible because  $v \gg u$  and  $v \gg w$ . That is, any reasonable assumptions concerning  $u = f(r)$  and  $w = f(r)$  are sufficient for the first approximation. The tangential velocity  $v$  dominates the momentum analysis. Keeping this fact in mind, we can idealize the  $w$  component for the cone shaped geometry analysis as follows:

$$w \neq f(\theta)$$

We assume equal vertical discharge to account for gradual decrease in cross-sectional area with  $z$ . For two concentric planes (1) and (2) at different heights, we have:

$$w_1 A_{s1} = w_2 A_{s2} \quad (51)$$

or

$$\frac{w_1}{w_2} = \left( \frac{r_2}{r_1} \right)^2 \quad (51)$$

but

$$r = r_w + Bz \quad (52)$$

where

$$r = r_w \text{ at } z = 0; -z = \text{downward}$$

so

$$w = \frac{w_w}{1 + 2 \frac{B}{r_w} z + \frac{B^2}{r_w^2} z^2} \quad (53)$$

and for the continuity equation,

$$\frac{\partial w}{\partial z} = - \frac{4w_w \left( \frac{B}{r_w} + \frac{B^2}{r_w^2} \right)}{\left[ 1 + 2 \frac{B}{r_w} z + \frac{B^2}{r_w^2} z^2 \right]^2} \quad (54)$$

that is,  $\frac{\partial w}{\partial z} = f(z)$  (54a)

Thus the continuity equation, equation 30, may be written for the cone-shaped geometry as follows:

$$\frac{1}{r} \frac{\partial}{\partial r} (ru) + \frac{\partial w}{\partial z} = 0 \quad (55)$$

Therefore,

$$\frac{1}{r} \frac{\partial}{\partial r} (ru) = -f(z) \quad (56)$$

And the integration is

$$ru = f(z) \quad (57)$$

The significance of this result is that the argument which led from equation 37 to equation 27,

$$v \frac{\partial}{\partial r} \left( \frac{1}{r} \frac{\partial}{\partial r} (ru) \right) = v \frac{\partial}{\partial r} \left( -f(z) \right) = 0$$

is unchanged.

So the arguments which lead to equations 40, 42 and 43 and to figure 7 to 10 are unchanged at the upper water surface (i.e., at  $z = 0$ ).

The practical limitation which may make this analysis, and to a lesser extent the previous sections IV-4 to IV-6, invalid is that we assumed at the outset that the surface indentation at the core is small compared with the vessel length  $l$ . It seems doubtful that this assumption is anything but crude in the proposed evaporator body designs.

Before passing to the bubble rise time analysis one result deserves emphasis. In each of the previous vortex flow analysis sections, the Eulerian residence time plotted in figure 10 was found

to be independent to the flow detail. It was a consequence only of continuity. Therefore any form of radial feed (with or without a tangential component of momentum; i.e., radial jet flows as the other extreme is also included) is roughly described by figure 10. A word of caution: the Eulerian flow field and the bubble or superheated fluid particle path may be appreciably different. (e.g., ref. 11). The turbulence and the neglected  $w$  component of the flow will tend to lower  $\tau_f$ . The only safe conclusion is that the average residence time of a fluid particle of superheated slurry at the surface is not greater than  $\tau_f$  of figure 10, and the actual  $\tau_f$  is probably less by as much as 50 percent.

#### V. BUBBLE ESCAPE RATE

Not only must the bubble growth rate be sufficiently rapid to meet design conditions within the time that the superheated slurry is exposed to the surface, but the buoyant forces acting on the bubble must be large enough for the vapor to escape within that time. This section briefly considers the bubble escape aspect of the problem.

The formulation of bubble mechanics is in principle very complex. For example, reference 12 discusses: internal vapor circulation affecting the interface drag, acceleration increasing the drag coefficient somewhat compared with measured steady-state values, and bubble shape distorting from non-uniform surface forces. However, it is entirely consistent with the previous heat transfer analysis (Sec. III) to assume that the bubble is a growing sphere of constant density  $\rho_v$  and to assume solid sphere drag relations apply. (Recall that the  $w_B$ , bubble rise velocity in the vertical, is measured relative to the moving fluid, so the large values of  $v$  do not disallow this assumption.) The application of Newton's Second Law takes the form:

$$\Sigma F = \frac{d}{dt} (m_v w_B) \quad (58)$$

Since the vapor mass in the growing bubble is changing with time, the

right hand side of equation 58 yields two terms!

$$\Sigma F = m_v \frac{dw_B}{dt} + w_B \frac{dm_v}{dt} \quad (58a)$$

The second term on the right ( $w_B \frac{dm_v}{dt}$ ) acts as an additional drag (just as in a rocket, the mass expulsion leads to a thrust). It is a straight forward procedure to solve for the bubble velocity  $w_B$  as a function of time after noting that:

$$\Sigma F = \text{Buoyant force} - \text{Surface Drag Force} \quad (58b)$$

and

$\frac{dm_v}{dt}$  and  $m_v$  are functions of time specified by the heat transfer analysis.

The buoyant force depends on the degree of swirl in the evaporator body. The slowest escape rate would result from gravity separation alone to a horizontal surface.

$$\text{Buoyant force} = \frac{4\pi R^3}{3} (\rho_L - \rho_v)g \quad (59)$$

The surface drag is a function of the bubble Reynolds number at any particular instant in time.

$$\text{Surface Drag} = \frac{C_D \pi R^2 \rho_L w_B^2}{2} \quad (60)$$

For example, when the bubble radius is somewhat less than  $10^{-1}$  mm, then the bubble is in the Stokes drag regime:

$$C_D = \frac{24}{\rho_L R w_B} \quad (R \lesssim 10^{-1} \text{ mm}), \quad (61)$$

However, at the later stages of the bubble growth when the bubble radius becomes slightly larger than 1 mm, then the drag coefficient approaches the turbulent flow value:

$$C_D \approx 0.39 \quad (R \gtrsim 1 \text{ mm}), \quad (62)$$

Now it is important to recognize that the heat transfer analysis is not appreciably modified by the transition to turbulent flow in the latter stages of its growth. That is, the bubble growth rate is largely completed in the laminar regime. Note that the data on real sphere growth (figs. 3a and 3b) extend to  $R \approx 1$  mm with good agreement with the heat transfer theory.

Although the "exact" solution of equation 58a is easily accomplished on a high-speed digital computer, a simple analytic solution cannot be found. Therefore, for the purposes of this preliminary study, we will make the following crude assumptions: (1) the overall escape time is controlled by the terminal velocity at the end of the bubble growth; (2) this terminal velocity will be in the turbulent regime; (3) the acceleration time to reach terminal velocity and the transition time through Stokes drag to turbulent regime are both negligible, (4) the added mass drag ( $w_B \frac{dm_v}{dt}$ ) is negligible. Of these, No. 4 is probably the worst. Numerically, this greatly simplified physical model leads to the following equation:

$$w_B \Big|_{\infty} = \sqrt{\frac{8 g R_m}{3 C_D}} \quad (63)$$

or

$$w_B \Big|_{\infty} = 0.85 \sqrt{R_m}$$

(ft/sec)                      (mm)<sup>1/2</sup>

And the estimated escape time  $\tau_E$  for any given liquid level is:

$$\Delta z = w_B \Big|_{\infty} \tau_E$$

or

$$\tau_E = \frac{\Delta z}{0.85 \sqrt{R_m}} \quad (64)$$

Several values of this estimated bubble escape time have been plotted on figure 12. The dashed line in this figure represents the predicted bubble growth time from the heat transfer analysis for the thermal

inlet conditions of Effect No. 4. That is, the dashed line on figure 12 came from the calculations summarized in figure 4. The solid lines are the escape time constant  $\tau_E$  for liquid heights indicated. The intersection of these lines determines the probable average bubble size at release. Clearly for a liquid level of 4 feet, the evaporator design must allow the superheated liquid to be near the liquid surface for more than 1 second if the design conditions of equilibrium is to be attained.

In any real evaporator, it seems doubtful that equilibrium will be approached as slowly as indicated. That is, several smaller bubbles will form faster (the maximum bubble size being limited by stability), but these bubbles will be escape-time limited falling into the shaded area of figure 12. This observation clearly points out the need for a more careful evaluation of equation 58 during the second phase of this study (i.e., the model tests described in section VII).

## VI. CONCLUSIONS OF PRECEDING ANALYSIS

Some critical comments are included herein as well as a brief summary of the preceding analyses.

Regardless of the volume of inlet feed from which the bubble forms, the times shown in figures 4 and 5 for single-bubble growths represent maximum values. That is, the slowest way to satisfy design vapor release is to draw superheat from a large volume of feed to form a single large bubble. Thermodynamically, many small bubbles drawing superheat from correspondingly small feed volumes leads to the same vapor release. Our analysis shows that the latter procedure is much faster. By matching the average bubble escape time calculation to the bubble formation time, it was possible to estimate the average bubble size at escape.

The calculations already presented on these dynamical characteristics of evaporation show that in Effect No. 4, we can expect maximum bubble sizes of about 10 mm at escape with both formation and escape taking place in much less than 10 seconds. It appears that any

reasonable feed inlet system and body shape will allow for the superheated slurry feed to be within 3 ft. of the surface for 10 seconds.

Furthermore, there appears to no function for forced vortex or tangential inlets unless very small bubbles are formed. As shown in figure 12, the need for vortex motion to aid escape rate will be a strong function not only of the depth of the feed "layer" but also of the inlet superheat. For Effect No. 4, the no-swirl escape rate seems sufficient but this observation is tentative and certainly requires experimental verification. Careful consideration of detailed model studies using radial inlet manifolds and new downheader geometries are strongly supported by the preceding analyses. However idealized the various sections of the analyses were, this conclusion seems beyond reasonable doubt. The suggested study might lead to very significant improvements in the elimination of wall crusting without jeopardizing the evaporation dynamics.

#### VII. PROPOSAL FOR MODEL STUDY

The complex nature of a mathematical treatment of flow conditions in an evaporator is apparent from preceding discussion and analysis. It is therefore proposed that it would be relatively simple to solve the problems for creating the proper environment within an evaporator body for maximum vapor release with a physical model. However, with a physical model, one needs to be aware of the laws of similitude and limitations of the results derived from a model in its application to the prototype.

Generally, two flow systems are said to be similar if they are geometrically, kinematically, and dynamically similar. In this instance a fourth requirement is that the model and prototype have thermal similarity. Geometric similarity exists between two systems if the ratios of all corresponding linear dimensions equal. Kinematic similarity is said to exist if the ratios of velocities and accelerations at all homologous points in a geometrically similar flow system are equal. Dynamic similarity exists if the ratio of forces at the same points in the systems are equal. It is necessary to include thermal

conditions in this model since pressure force also depends upon the thermal condition in addition to viscous, gravitational and inertial forces.

The pressure coefficient or Euler Number is a dependent variable for once the inertial, gravitational, viscous and thermal forces are fixed, the corresponding pressure is fixed. The ratio of inertial forces to gravitational forces is expressed as

$$F = \frac{\rho v^2}{\gamma L}$$

where

$$\begin{aligned} \rho &= \text{fluid density} \\ v &= \text{fluid velocity} \\ \gamma &= \text{specific fluid weight} \\ L &= \text{characteristic linear dimension} \end{aligned}$$

and  $F$  is a dimensionless number called the Froude number. The rate of inertial forces to viscous forces is expressed as:

$$R_e = \frac{\rho L v}{\mu}$$

where  $\mu$  = dynamic viscosity of the fluid

and  $R_e$  = dimensionless Reynolds number.

Thermal conditions can be included in the "cavitation" number

$$C = \frac{\Delta P}{\frac{\rho v^2}{2g}}$$

such that for equal cavitation numbers in model and prototype the vapor release characteristics should be similar.

In a study of evaporator performance it should be only necessary to model a single effect. However different the thermodynamic conditions may be in the other effects, it should not be necessary to alter basic geometry of the evaporator bodies.

#### 1. Objective of the Model Study

The objective of the model study is to develop a fixed evaporator body geometry with all its auxiliary parts to create a fluid environment within the evaporator body such that:

- (a) Maximum vapor release is attained ,
- (b) Minimum short-circuiting of the superheated fluid occurs, which is intimately allied with objective 1.
- (c) Crystal growth and homogeneous or turbulent mixing of the crystals in the slurry is achieved.
- (d) Minimum solids and liquor carry-over occurs with the evacuated vapor.
- (e) Crystal-free concentrated brine can be extracted from the evaporator.
- (f) Minimize or eliminate salt crusting on the internal evaporator pan walls.

## 2. Proposed Method of Study

Alternative I - Modeling an evaporator involves both Froude and Reynolds laws of similitude. While theoretically it is possible to derive relationships which include both factors, practically it is impossible because a fluid to be used in the model which has the required density and viscosity characteristics does not exist. Obviously then, some other means must be used to develop an acceptable model.

The free surface in the evaporator indicates that flow in the evaporator is dominated by gravitational and inertial forces so that the Froude criteria prevails. Within the confines of the closed conduits the Reynolds number prevails since viscous forces predominate. It is proposed in this model, that the Froude criterion be used to determine the geometric scale and hydraulic relationships. The scale must be chosen sufficiently large so that viscous forces are minimized in relative influence on the pressure forces. The length of piping for the model must be altered from strict geometrical relationships so that the pressure gradient on the model is similar to that of the prototype. It will be necessary to distort the thermal effects (heat exchange) in the model so that vapor release in model and prototype are similar. If the same fluid is used in the model as that in the prototype then additional driving force in vapor

release must be achieved with a greater temperature differential in the heat exchanger. It is suggested that the geometric relationship between model and prototype be about 1:5 or 1:6.

Consistent with previous discussions with representations of the Stearns-Roger Manufacturing Company, it is proposed that the model be constructed by the Stearns-Rogers Manufacturing Company. It will be necessary to provide the model of the evaporator body, the recirculating pumping units, the heat exchange units and a vapor evacuator and condenser. A steam generator may be required in the list of equipment to be supplied. If possible it is the intent to utilize plant steam for the model which will be available between the months of October to April. General design of the model should be the responsibility of the research personnel. Specific alteration of entrance and pump exit geometries will be the responsibility of the researchers. Major reconstruction will be the responsibility of Stearns-Roger Manufacturing Company.

It is proposed that experimental study begin with the selected vendor's design. When study of that design progresses to a point where maximum vapor release is obtained from the model, modifications should be made to study a different flow environment within the evaporator. If the vendor's selected design happens to involve rotating fluid motion within the evaporator, the second part of the study will be the level surface flow environment and vice versa.

Alternative II - Assuming that theoretical computations can be relied upon to determine vapor release from the superheated liquor, an alternative proposal is to model only the flow conditions within the evaporator body. The fluid in this model can be water and the thermal effects can be neglected. If the fluid entrance is adjusted to prevent short circuiting, other physical aspects within the evaporator remaining equal, this would normally lead to maximum vapor release. Since this model would not involve the thermodynamic aspects of the total problem a less complex model can be used. Similitude of flow conditions can be satisfactorily achieved by adherence to the Froude criterion; and the results would be qualitative.

As in the first model proposed, experimentation would begin with the vendor's design and alterations can be made from results of the experiments. Determination of minimum short circuiting can be accomplished with use of non-soluble dye injected into the entrance flow. The relative differences of flow conditions between rotating flow and level surfaces with both above and below surface flow entrances will be qualitatively evaluated. The effect on problems at the suction side of the recirculating pump can be experimentally solved as this problem should be independent of thermodynamic effects. Salt crystals in this model could be represented by insoluble particles added to the flow with fall velocity of the particle in the model fluid scaled to the fall velocity of salt crystals in the prototype brine. The latter would be calculated from available data.

This alternative model would also be constructed by the Stearns-Roger Manufacturing Company from general design determined by the research personnel. Because water will be used, the model need not involve corrosion resistant metal. It would be advantageous to have this model constructed from clear plexiglas so that flow within the evaporator can be readily observed. The model will include the evaporator body, three or four pumping units and a vacuum pump to reduce the pressure above the surface in the evaporator. Alterations to the evaporator will be made by the researchers.

### 3. Time Estimates

Alternative I - This model study involves careful control of the many variables involved in the total process, hence each experimental test will require considerable time. Without specific precedence it is estimated that about two months will be required for design and detailing the model for construction, and three months of testing time will be required for each of the two basic flow motions proposed for study. These estimates will be subject to closer evaluation after model details are studied and certainly after some tests have been undertaken. These time estimates do not include time for model construction or major reconstruction.

Alternative II - Total time including time for design and tests with alterations is estimated to be about five months not consecutive. Design time with detailed drawings for construction is estimated to require one month with two months required for testing each of two basic fluid environment cases, i.e. rotating fluid body, and level surface fluid body. Minor alteration times are included in this estimate.

4. Cost Estimates:

## Alternative I

A. Direct Costs

## 1. Salaries

|  |   |              |          |
|--|---|--------------|----------|
| Principal researcher 8 mos.<br>at 1100/mo. | = | \$ 8,800     |          |
| Co-Researcher 6 mos. at<br>1100/mo.        | = | 6,600        |          |
| Advisors 3 mos. at 1200/mo.                | = | <u>3,600</u> | \$19,000 |

## 2. Labor

|  |   |              |          |
|--|---|--------------|----------|
| Graduate Assistants (2) 8 man mos.<br>at 600/mo. | = | 4,800        |          |
| Secretarial 100 hrs. at 2.50/hr                  | = | 250          |          |
| Shop 500 hrs at 3.50/hr                          | = | <u>1,750</u> | \$ 6,800 |

3. Materials (welding, lumber,  
misc.)

= 2,000

## 4. Miscellaneous

|  |   |     |  |
|--|---|-----|--|
| Travel (local travel in<br>acquisition of materials) |   | 100 |  |
| Acquisition of literature                            | = | 200 |  |

## 5. Report Preparation

|                       |   |            |          |
|-----------------------|---|------------|----------|
| Photographic supplies | = | 100        |          |
| Reproduction          | = | <u>300</u> | \$ 2,700 |

B. Indirect Costs

|  |               |          |
|--|---------------|----------|
| Overhead at 75 percent of salaries and labor | <u>19,350</u> | \$19,350 |
|--|---------------|----------|

TOTAL COST

\$47,850

4. Cost Estimates (cont)

## Alternative II

A. Direct Costs

## 1. Salaries

|  |   |              |          |
|--|---|--------------|----------|
| Principal research 5 mos.<br>at 1100/mo. | = | \$ 5,500     |          |
| Co-Researcher 4 man mos.<br>at 1100/mo.  | = | 4,400        |          |
| Advisors 2 man mos. at 1200/mo.          | = | <u>2,400</u> | \$12,300 |

## 2. Labor

|  |   |              |          |
|--|---|--------------|----------|
| Graduate Assistants (2) 5 man<br>mos. at 600/mo. | = | 3,000        |          |
| Secretarial 100 hrs at 2.50/hr                   | = | 250          |          |
| Shop 500 hrs at 3.50/hr                          | = | <u>1,750</u> | \$ 5,000 |

3. Materials (plastic, steel,  
lumber)

= 4,000

## 4. Miscellaneous

Travel (local) = 100

## 5. Report Preparations

|                       |   |            |          |
|-----------------------|---|------------|----------|
| Photographic supplies | = | 300        |          |
| Reproduction          | = | <u>300</u> | \$ 4,700 |

B. Indirect Costs

|  |  |               |          |
|--|--|---------------|----------|
| Overhead at 75 percent of salaries and labor |  | <u>12,975</u> | \$12,975 |
|--|--|---------------|----------|

|            |  |  |                 |
|------------|--|--|-----------------|
| TOTAL COST |  |  | <u>\$34,975</u> |
|------------|--|--|-----------------|

5. General Comment on Proposal

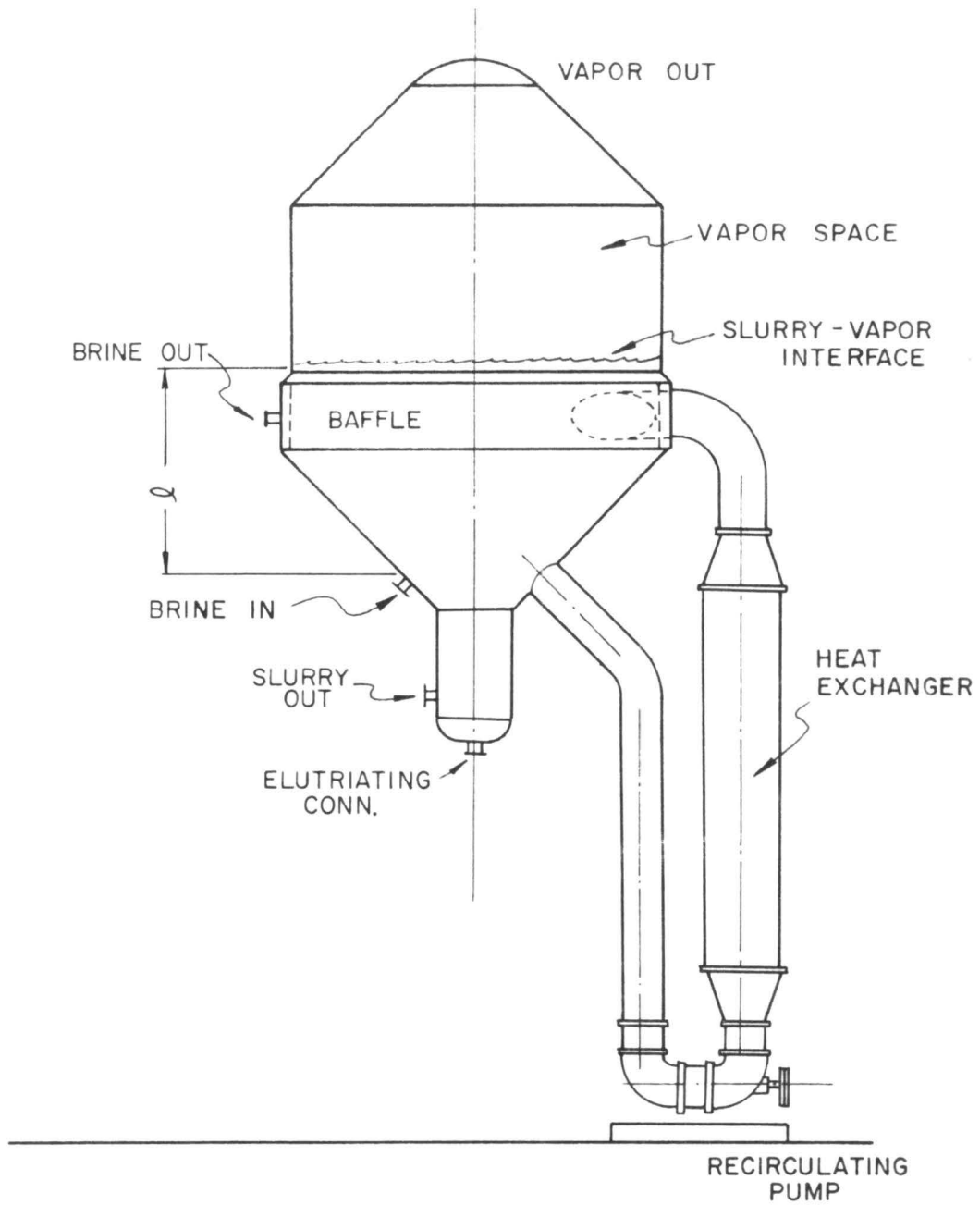
This proposal for model study should be considered preliminary. The model study outline is intended only as a guide to assist the Stearns-Roger Manufacturing Company in determining whether a model study is feasible. Should a model investigation be seriously considered it is suggested that one of the alternative plans to be selected and a more firm proposal be prepared on that plan subsequent to further detailed discussion. These proposed time schedules and cost estimates should not therefore be considered binding to the Colorado State University Research Foundation at this time.

## VIII. ACKNOWLEDGEMENTS

The writers hereby acknowledge the participation of Mr. R. L. Steele, Dr. V. M. Yevdjevich and Dr. D. B. Simons for their valuable contributions not only towards preparation and review of this report, but also for their knowledge and ideas presented in several group discussions on the evaporator problem. The writers and Dr. Yevdjevich wish to express appreciation to Mr. R. W. Wrighton and his staff at the International Salt Company at Watkins Glen, New York for permission to inspect their evaporators at the plant and to Pittsburgh Plate Glass Company and Stearns-Roger Manufacturing Company for making the inspection trip possible. Through discussions with personnel of the International Salt Company the participants of this study were able to determine much of the physical significance of total problems expressed inherently in this report.

Reference List:

1. Paul, B.: "Compilation of Evaporation Coefficient," Journal of American Rocket Society, Sept. 1962, pp. 1321-1328.
2. Plesset, M. S. and Zwick, S. A.: "A Nonsteady Heat Diffusion Problem with Spherical Symmetry," J. Appl. Physics, Vol. 23, (1952), p. 95.
3. Plesset, M. S. and Zwick, S. A.: "The Growth of Vapor Bubbles in Superheated Liquids," J. Appl. Physics, Vol. 25, (1954), p. 493.
4. Dergarabedian, P.: "The Rate of Growth of Vapor Bubbles in Superheated Water," J. Appl. Mechanics, Vol. 20, (1953), p. 537.
5. Dergarabedian, P.: "Observations on Bubble Growth in Various Superheated Liquids," J. Fluid Mechanics, Vol. 2, (1960), p. 39.
6. Lamb, G.: "Hydrodynamics," Dover Publications, New York, 1945.
7. Gartshone, I. S.: "Recent Work in Swirling Incompressible Flow," Nat. Res. Council of Canada, Aero. Report LR-343, June, 1962.
8. Einstein, H. A., and Li, H.: "Steady Vortex Flow in a Real Fluid," Preprints of 1951 Heat Transfer and Fluid Mechanics Institute, Stanford Univ. Press, 1951. Also La Houille Blanche, Vol. 10, (1955), pp. 483-496.
9. Li, H.: "Steady Vortex Flow in a Real Fluid," M.S. Thesis, U. of Calif., (Berkeley) 1950 (?).
10. Deissler, R. G. and Perlmutter, M.: "Analysis of the Flow and Energy Separation in a Turbulent Vortex," Int. J. Heat Mass Transfer, Vol. 1, (1960) p. 173-191.
11. Baldwin, L. V. and Mickelsen, W. R.: "Turbulent Diffusion and Anemometer Measurements," Proc. A.S.C.E., J. Eng. Mech. Div., EM2, April 1962.
12. Hughes, R. R. and Gilliland, E. R.: "The Mechanics of Drops," Reprints of the 1951 Heat Transfer and Fluid Mechanics Institute, Stanford University Press (1951).



SKETCH A  
 ELEVATION VIEW OF CYLINDRICAL EVAPORATOR

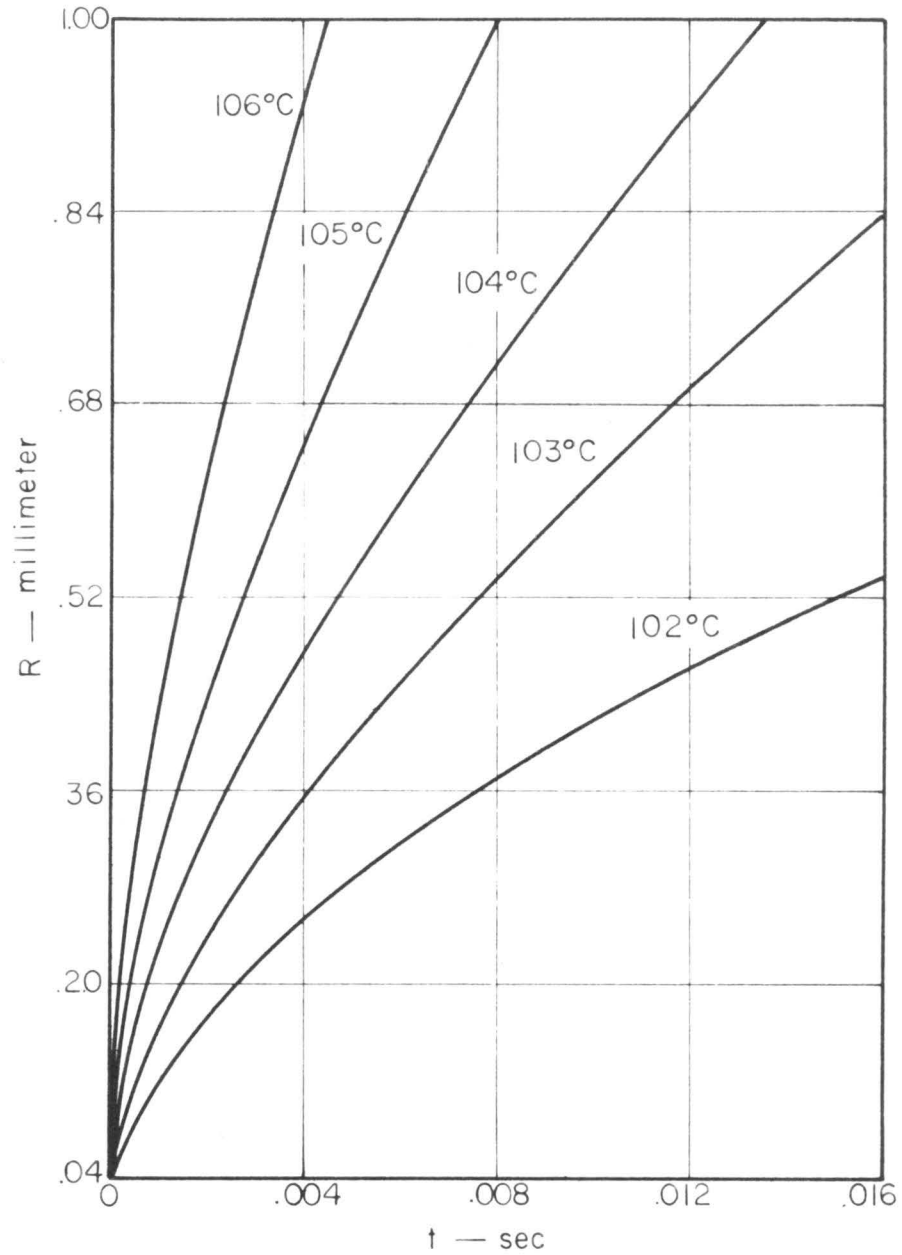


FIG. 1 CALCULATED BUBBLE RADIUS VS. TIME CURVES AT THE INDICATED SUPERHEAT TEMPERATURES IN WATER AT 1 ATMOS. (Ref. No. 3)

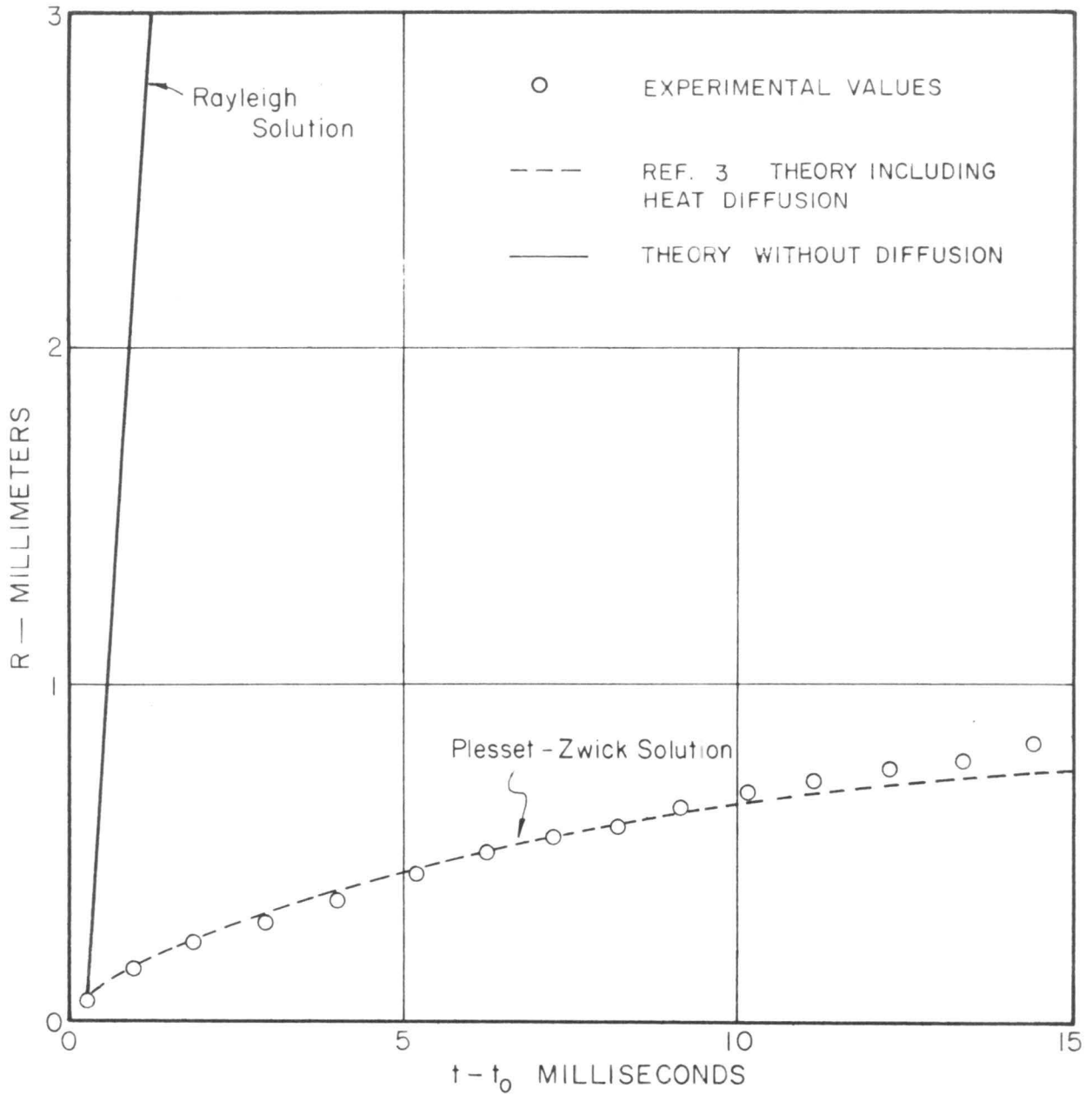


FIG. 2 EXPERIMENTAL VAPOR BUBBLE GROWTH RATE IN 103.1°C SUPERHEATED WATER AT 1 ATM. (Ref. No. 3)

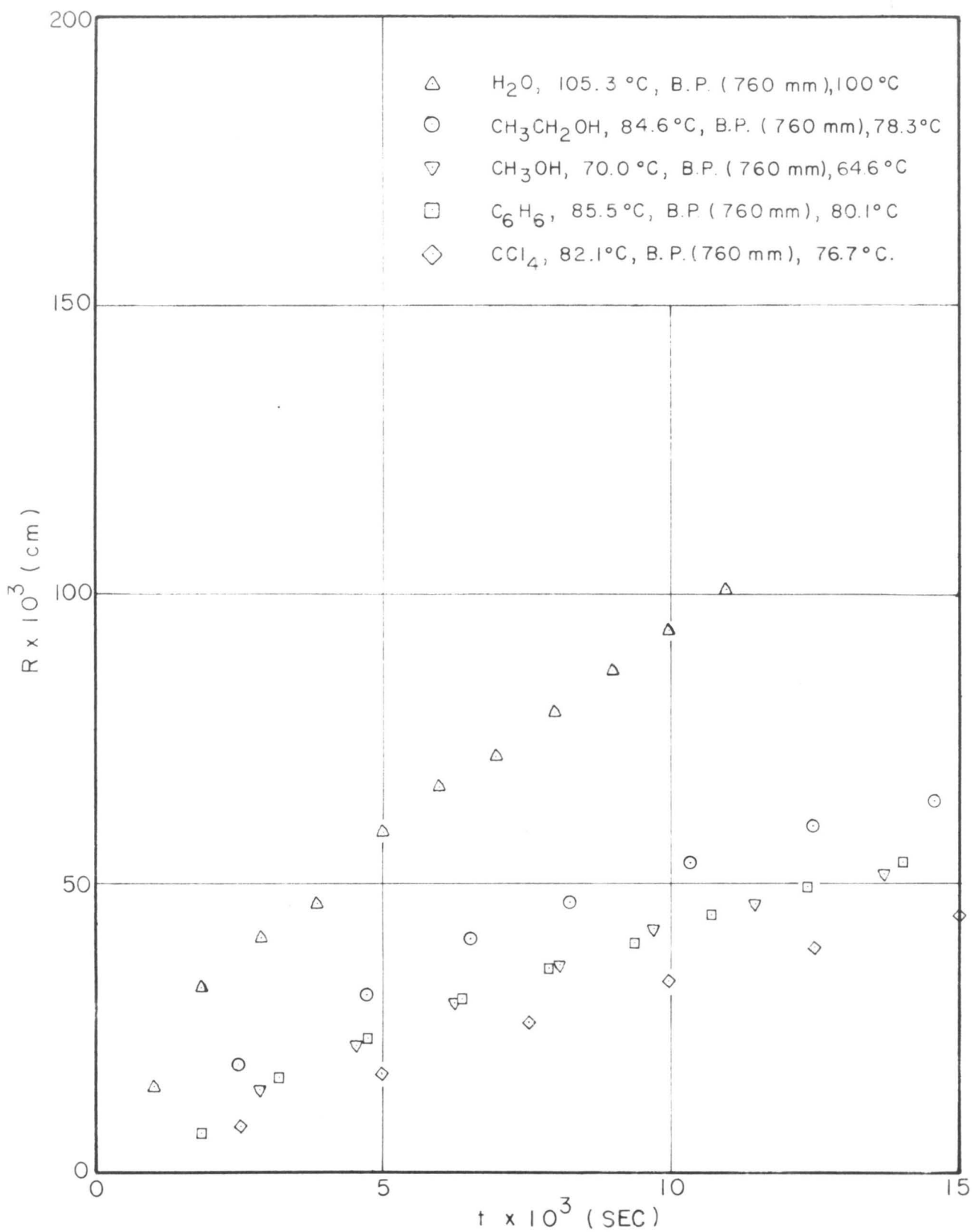


FIG. 3a EXPERIMENTAL VAPOR BUBBLE GROWTH RATE (Ref.No.5)

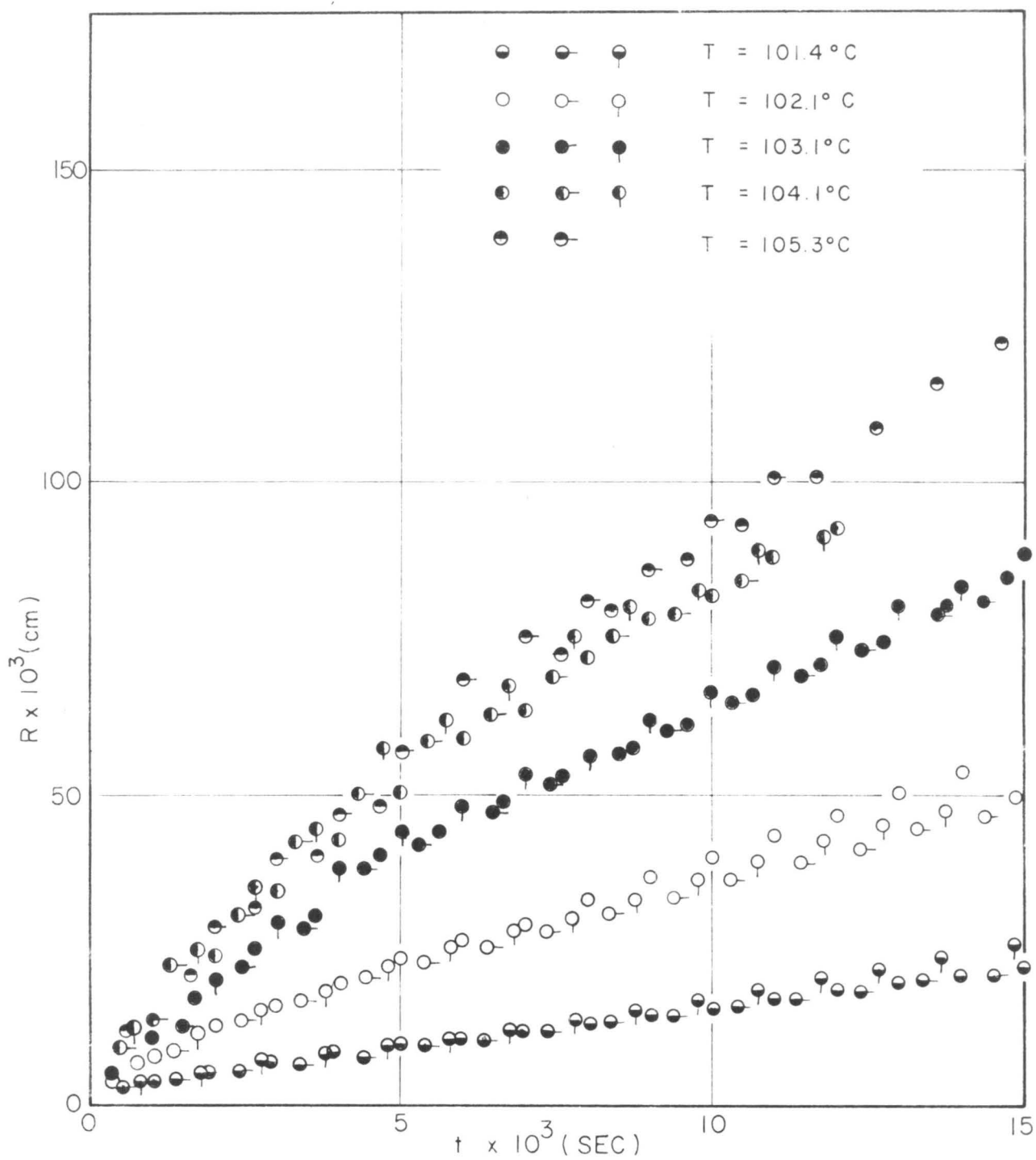
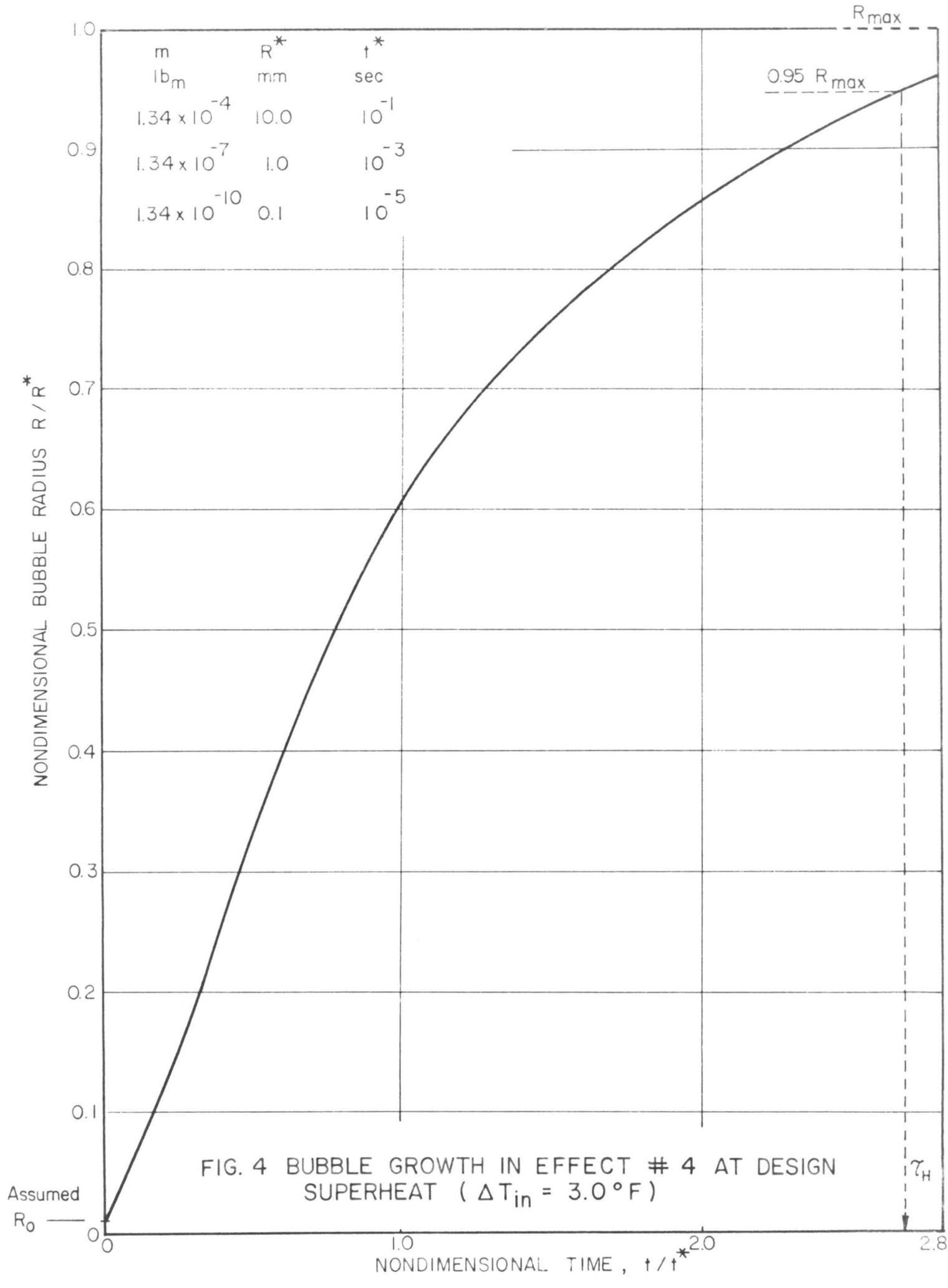


FIG. 3 b EXPERIMENTAL DATA FOR BUBBLE GROWTH IN SUPERHEATED WATER AT 1 ATM. AMBIENT PRESSURE ( Ref. 4 P. Dergarabedian)



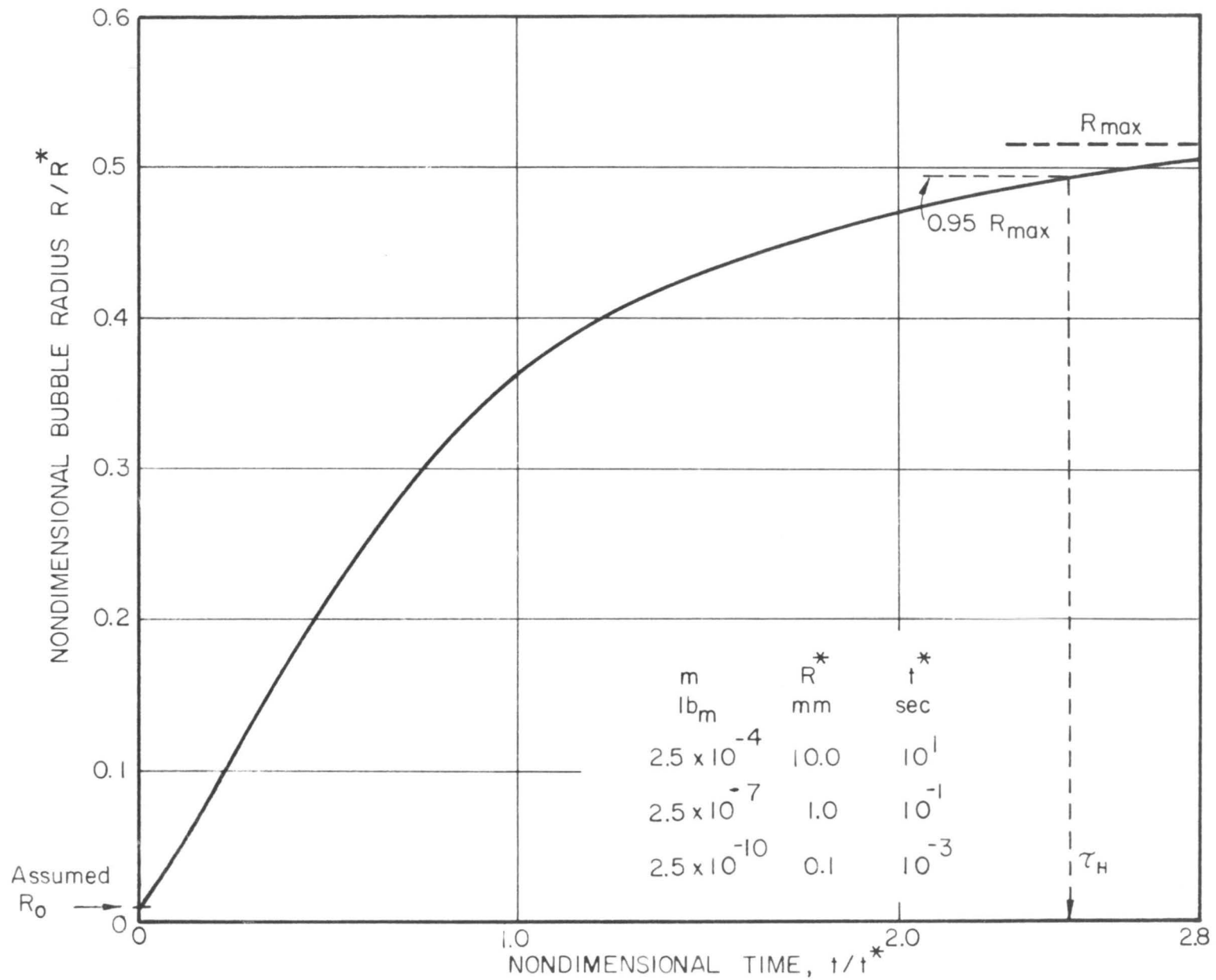


FIG. 5 BUBBLE GROWTH IN EFFECT #4 AT 0.73 TIMES DESIGN SUPERHEAT ( $\Delta T_{in} = 2.2^\circ F$ )

ASSUMED VALUES:

$$r_o = \text{EQUIVALENT DRAIN DIAMETER} = \sqrt{\frac{A_{\text{Tot, out}}}{\pi}} = \sqrt{\frac{3 \times \pi \times (42/12)^2}{4 \pi}} = 3.03 \text{ ft}$$

$$r_w = \text{OUTER RADIUS} = 16.8 \text{ ft}$$

$$u_o = \text{RADIAL VELOCITY AT DRAIN} = \frac{Q}{2\pi r_o l} = \frac{333}{2\pi \times 3.03 \times 20} = 0.875 \text{ ft/sec}$$

$$v_w = \text{TANGENTIAL VELOCITY AT WALL} = \frac{Q}{A_{\text{Tot, in}}} = \frac{333}{3 \times \pi/4 \times (48/12)^2} = 8.75 \text{ ft/sec}$$

GEOMETRY:

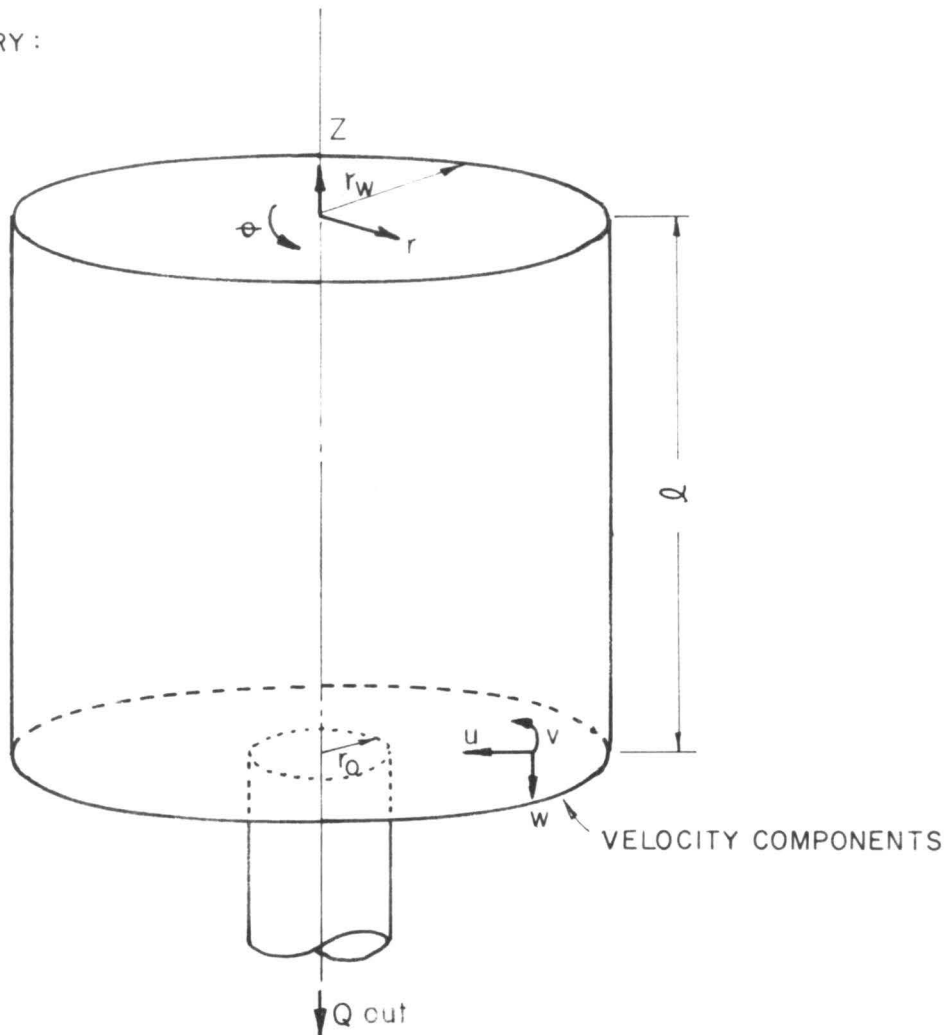


FIG. 6 SKETCH FOR VORTEX FLOW ANALYSIS

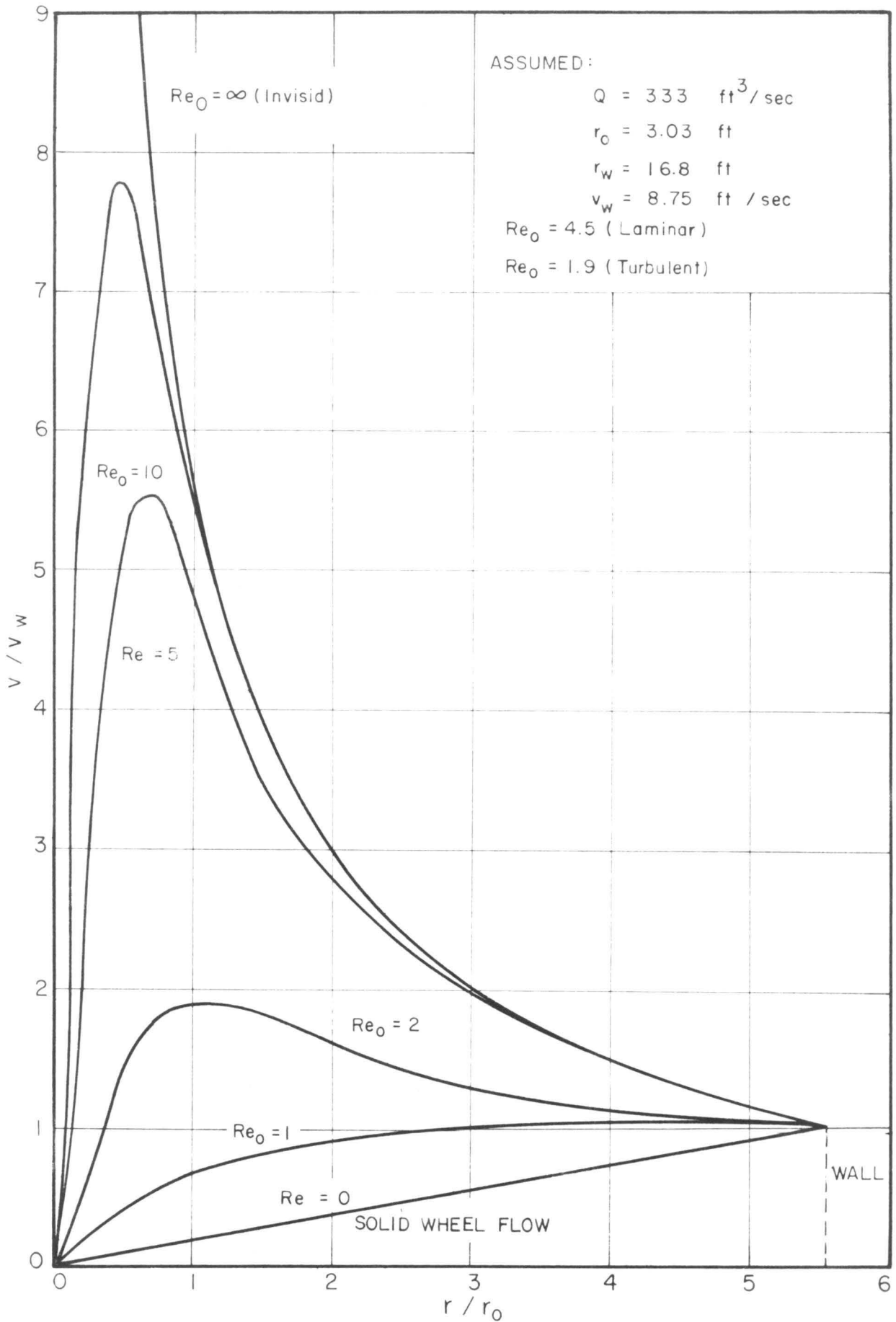


FIG.7 TANGENTIAL VELOCITY FIELD IN REAL VORTEX FLOW

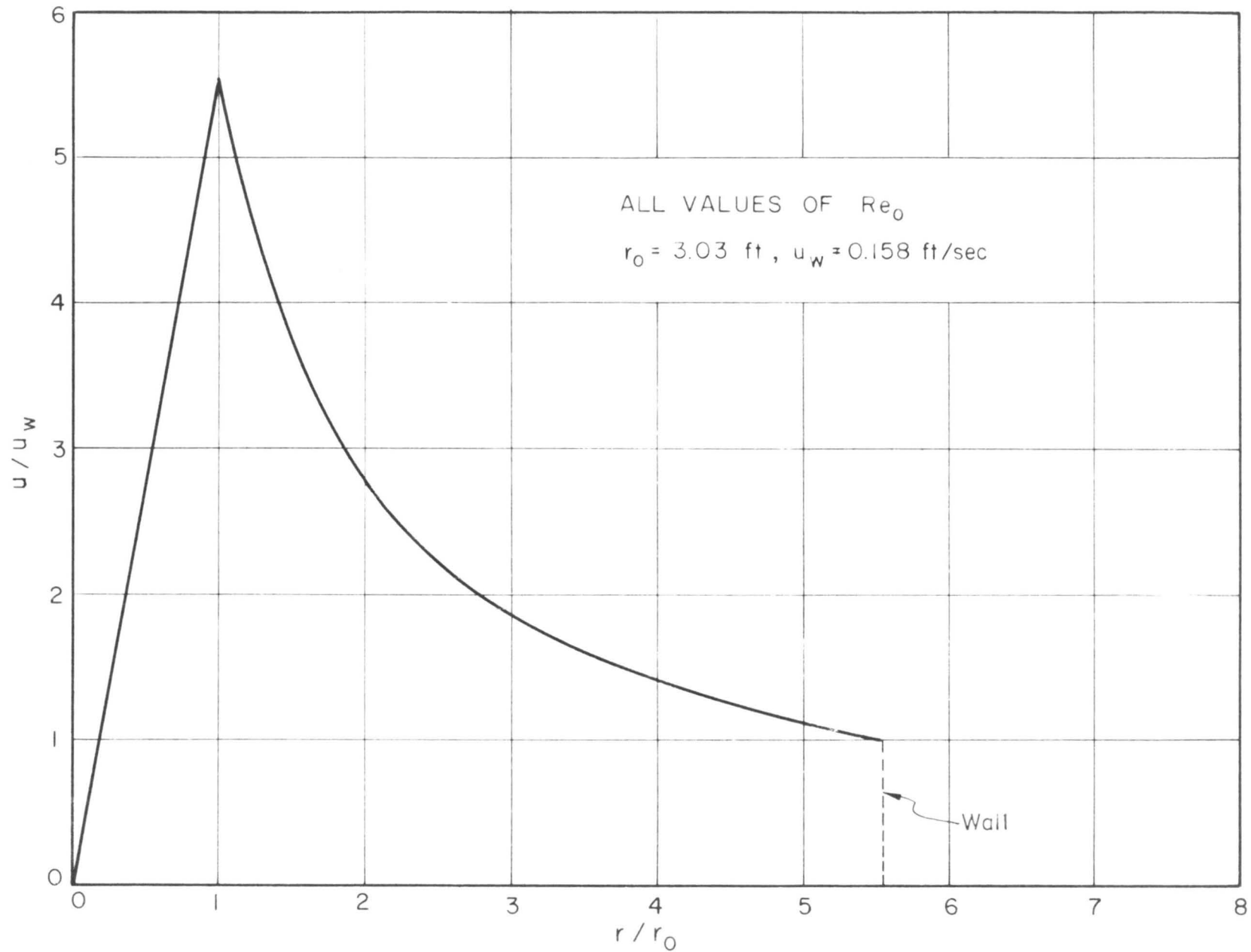


FIG. 8 RADIAL VELOCITY FIELD IN A VORTEX FLOW

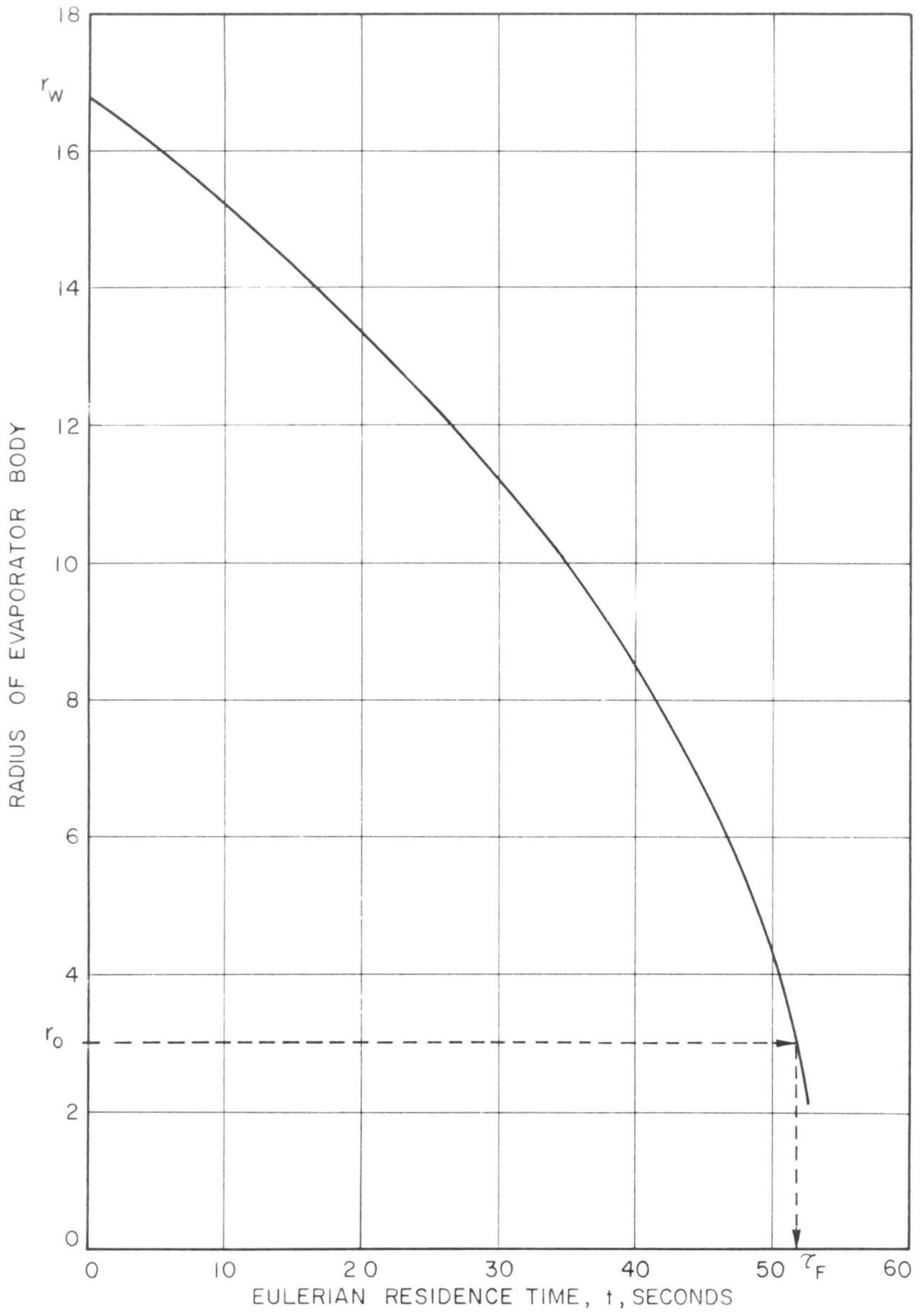


FIG. 9 EULERIAN RESIDENCE TIME IN A VORTEX FLOW

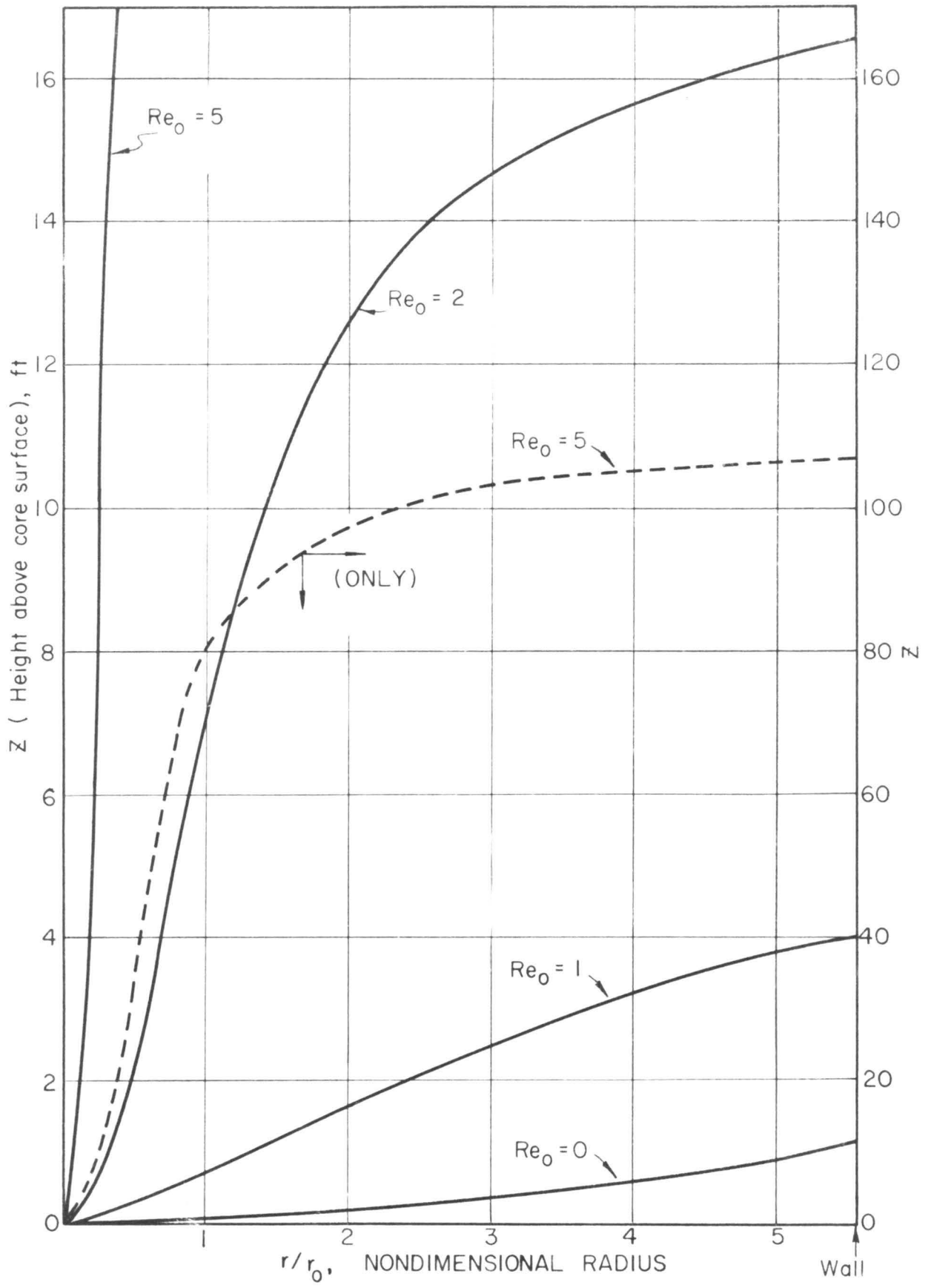


FIG. 10 SHAPE OF WATER SURFACE

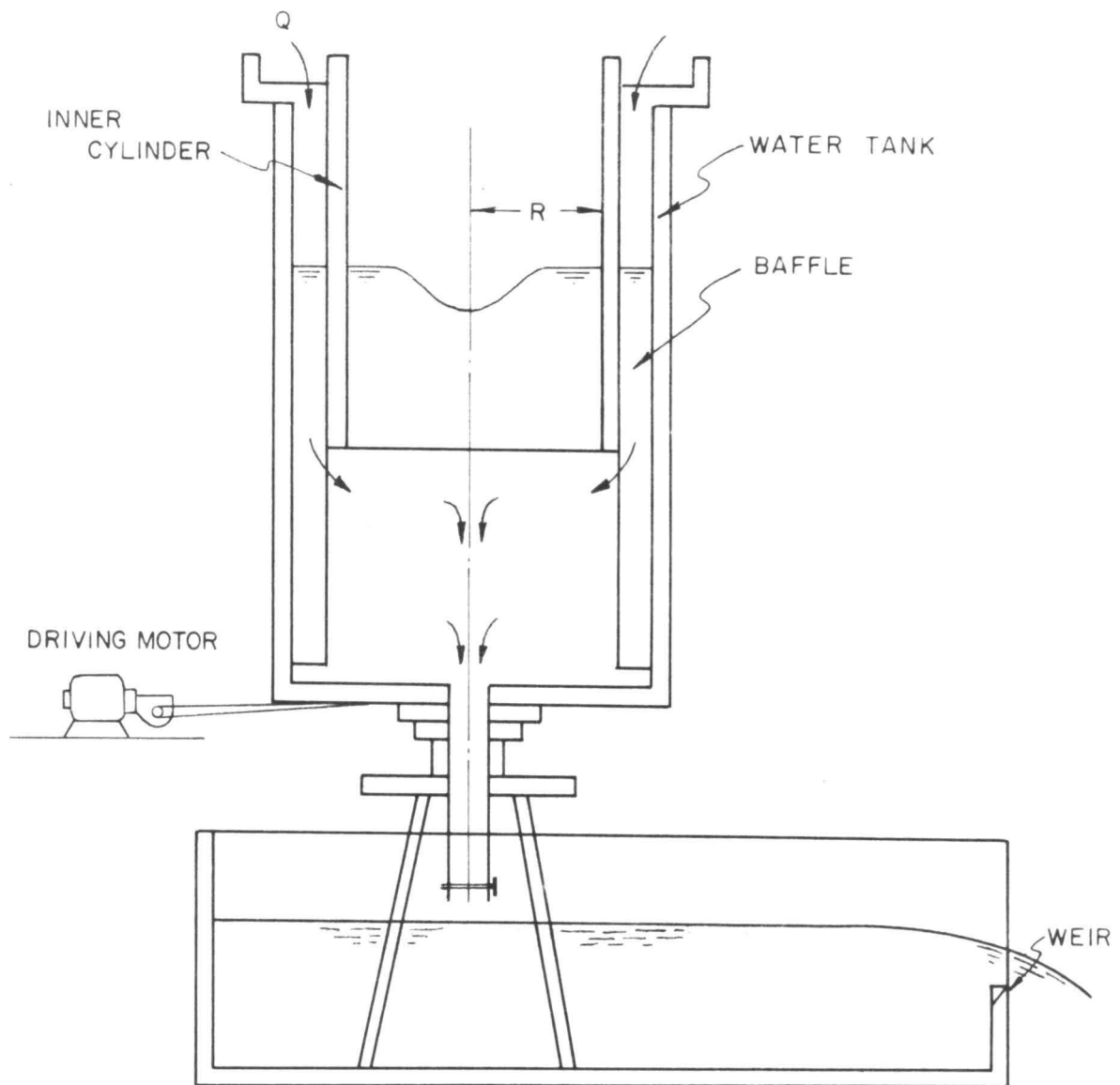


FIG. 11 EXPERIMENTAL TANK FOR GENERATION OF VORTICES IN A REAL FLUID ( Ref. No.8 )

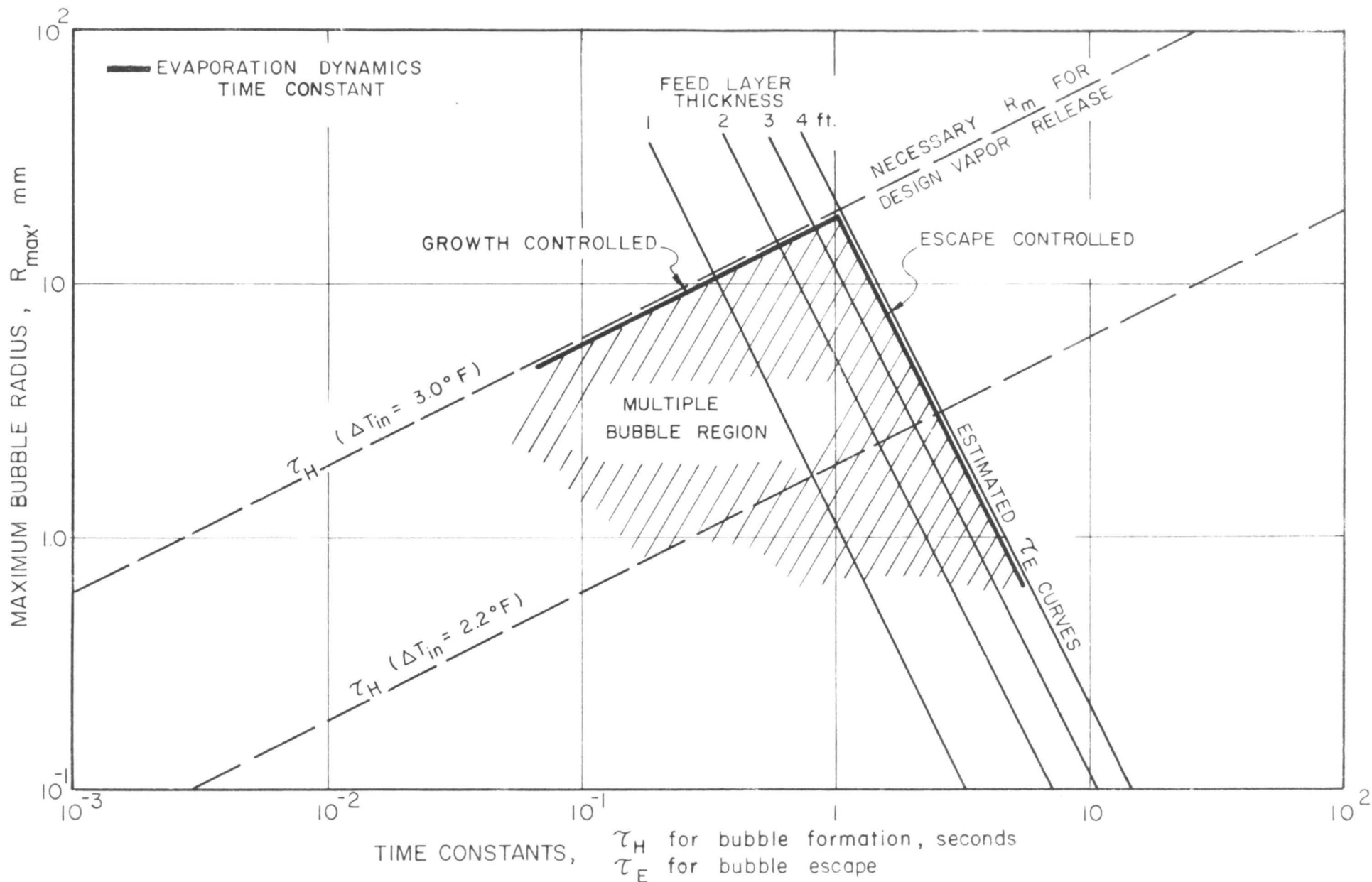


FIG. 12 SUMMARY OF EVAPORATION DYNAMICS WITHOUT SWIRL